② **LEVEL** II

THE ANODIC STRIPPING VOLTAMMETRIC ANALYSIS OF
CHROMIUM USING THE HANGING MERCURY DROP ELECTRODE

JOHN EDWARD FUGATE 1LT
HQDA, MILPERCEN (DAPC-OPP-E)
200 Stovall Street
Alexandria, VA 22332

Final Report
23 APR 1981

Approved For Public Release;
Distribution Unlimited

DTIC
ELECTE
S
JUN 10 1981
D

B

A Thesis Submitted to Western Kentucky University,
Bowling Green, KY in Partial Fulfillment
of the Requirements for the Degree of
Master of Science

81 6 02 046

REPORT DOCUMENTATION PAGE		READ INSTRUCTIONS BEFORE COMPLETING FORM
1. REPORT NUMBER	2. GOVT ACCESSION NO. AD-A100 010	3. RECIPIENT'S CATALOG NUMBER
4. TITLE *(and Subtitle)* THE ANODIC STRIPPING VOLTAMMETRIC ANALYSIS OF CHROMIUM USING THE HANGING MERCURY DROP ELECTRODE		5. TYPE OF REPORT & PERIOD COVERED Final Report 23 APR 81
		6. PERFORMING ORG. REPORT NUMBER
7. AUTHOR*(s)* JOHN EDWARD FUGATE		8. CONTRACT OR GRANT NUMBER*(s)*
9. PERFORMING ORGANIZATION NAME AND ADDRESS Student, HQDA, MILPERCEN ATTN: DAPC-OPP-E 200 Stovall St., Alexandria, VA. 22332		10. PROGRAM ELEMENT, PROJECT, TASK AREA & WORK UNIT NUMBERS
11. CONTROLLING OFFICE NAME AND ADDRESS HQDA, MILPERCEN, ATTN: DAPC-OPP-E 200 Stovall Street Alexandria, VA 22332		12. REPORT DATE 23 APR 81
		13. NUMBER OF PAGES 67
14. MONITORING AGENCY NAME & ADDRESS*(if different from Controlling Office)*		15. SECURITY CLASS. *(of this report)* UNCLASSIFIED
		15a. DECLASSIFICATION/DOWNGRADING SCHEDULE

16. DISTRIBUTION STATEMENT *(of this Report)*

Approved for public release; distribution unlimited

17. DISTRIBUTION STATEMENT *(of the abstract entered in Block 20, if different from Report)*

18. SUPPLEMENTARY NOTES

This document is a thesis prepared from research performed at Western Kentucky University, Bowling Green, KY.

19. KEY WORDS *(Continue on reverse side if necessary and identify by block number)*

Anodic Stripping Voltammetry
Trace Analysis of Chromium
Hanging Mercury Drop Electrode

20. ABSTRACT *(Continue on reverse side if necessary and identify by block number)*

The Hanging Mercury Drop Electrode (HMDE) is used in the anodic stripping analysis of ppm concentrations of chromium. The effects of such parameters as ionic strength, polymeric film formation, and the use of the chromate-sodium acetate standard are interpreted in terms of the electrochemical and physical properties of chromium in the +3 and +6 oxidation states.

DD $_{1 JAN 73}^{FORM}$ 1473 EDITION OF 1 NOV 65 IS OBSOLETE

THE ANODIC STRIPPING VOLTAMMETRIC ANALYSIS OF

CHROMIUM USING THE HANGING MERCURY DROP ELECTRODE

A Thesis

Presented to

the Faculty of the Department of Chemistry

Western Kentucky University

Bowling Green, Kentucky

In Partial Fulfillment

of the Requirements for the Degree

Master of Science

by

John Edward Fugate

23 APRIL 1981

THE ANODIC STRIPPING VOLTAMMETRIC ANALYSIS OF

CHROMIUM USING THE HANGING MERCURY DROP ELECTRODE

Recommended _4-13-1981_
(DATE)

John T. Riley
Director of Thesis

Laurence J. Boucher

Robert D. Farina

Approved _April 23, 1981_
(DATE)

Elmer Gray
Dean of the Graduate College

Acknowledgements

I wish to express my sincere gratitude to the faculty of Western Kentucky University's Chemistry Department and, in particular to my research director, Dr. John T. Riley who gave unselfishly of his time and knowledge. I also express my thanks to Dr. Laurence Boucher and Dr. Robert Farina, the other members of my research committee. Finally, I would like to recognize my wife, Kay, and my son John Byron, for their patience, love, and understanding during my stay here at Western.

TABLE OF CONTENTS

LIST OF FIGURES

LIST OF TABLES

THE ANODIC STRIPPING VOLTAMMETRIC ANALYSIS OF

CHROMIUM USING THE HANGING MERCURY DROP ELECTRODE

John Edward Fugate   May 1981   67 Pages

Directed by: John T. Riley, Laurence Boucher, Robert Farina

Department of Chemistry   Western Kentucky University

The Hanging Mercury Drop Electrode (HMDE) is used in
the anodic stripping analysis of ppm concentrations of
chromium. The effects of such parameters as ionic strength,
polymeric film formation, and the use of the chromate-sodium
acetate standard are interpreted in terms of the electro-
chemical and physical properties of chromium in the +3 and
+6 oxidation states.

I. INTRODUCTION

A. Problems and Methods of Trace Analysis

Present problems in technology, the bio-medical fields, and environmental protection require determinations of ever-decreasing concentrations of substances in increasingly complex chemical environments. These problems place increasing demands on all methods of trace analysis.

Generally, trace analysis requires the solution to three problems: (1) achieving sufficient sensitivity of the method, (2) obtaining selectivity in determinations where potentially interfering substances may be orders of magnitude more concentrated than the analyte(s), (3) obtaining pure chemicals and mastering work with extremely dilute solutions in which the amount of dissolved substances may diminish with time.

Many analytical methods have been developed to deal with these problems, the most sensitive of which include radio-chemical methods, UV fluorescence, emission spectral analysis and gas chromatography. Radiochemical methods (activation analysis and tracer techniques) have detection limits, in optimal cases, of 10^{-21} grams. Also, the accuracy and precision of the analysis is dependent on the number of disintegrations, both of which can be improved by merely prolonging the counting time. However, the sensitivity of activation analysis is variable for those metals having low activation cross sections (e.g. Bi, Pb, Tl, and Hg). A similar decrease in sensitivity occurs with tracer analysis in the case of

nuclides with very long half-lives. UV fluorescence and
emission spectral analysis attain detection limits of 10^{-15}
grams and 10^{-12} grams, respectively, but suffer from low
accuracy and precision due to considerable matrix effects on
the determination. Gas chromatography attains a similar
sensitivity and is both a separational and detection method.
However, it is limited in application to substances with
relatively low boiling points.

A number of methods can be used for analysis in the
range from about 10^{-6} to 10^{-10} grams including the spectro-
photometric methods of atomic absorption and fluorescence,
and the methods of stripping analysis as outlined by Vydra
et al. in "Electrochemical Stripping Analysis."[1] While
optical methods are usually very sensitive and have a broad
range of application, the instrumentation is costly and sen-
sitive to matrix effects. Stripping methods, on the other
hand, are more sensitive for certain substances, instrumen-
tation is relatively inexpensive, and less sensitive to matrix
effects. Also electrolytic methods have an advantage in their
much more exact and fully developed theoretical background
due, chiefly, to the extensive polarographic literature.

B.   The Electrochemical Approach to Trace Analysis

Classical polarographic methods have detection limits of
about 10^{-5}M, or on the order of micrograms of analyte. This
detection limit is determined by the ratio of the electrolytic
current to the background current, which is the sum of the
currents due to the solution's impurities, charging of the

electrical double-layer and electronic noise in the measuring circuit.

The sensitivity of classical methods can be increased by suppressing the electronic noise level, or by measuring instantaneous concentrations in the diffusion layer of the electrode. Increasing the flux of the depolarizer (analyte) to the electrode by stirring the solution or rotating the electrode can increase the sensitivity an order of magnitude, but reproducibility of data deteriorates somewhat.

To increase the sensitivity by several orders of magnitude, a stripping technique must be used. The stripping method consists of preconcentration of a very dilute sample for a specified period of time. This preconcentration or pre-electrolysis step can be carried out directly in the solution on which the measurement itself will be made. Thus, a slow, tedious, and often mistake-prone separation step is eliminated. After pre-electrolysis at constant potential, the substance is then "stripped" from the electrode by the reverse electrolytic process.

The description above is for a general stripping method. Anodic stripping voltammetry (ASV) entails, specifically, the selection of a pre-electrolysis potential which is more negative (cathodic) than the half-wave reduction potential ($E_{\frac{1}{2}}$) for the particular metal. Pre-electrolysis is carried out at this constant potential while the solution is stirred. Usually, pre-electrolysis times do not exceed ten minutes, but may reach as high as thirty minutes in some cases. After pre-electrolysis, the stirring is stopped and the solution is

allowed to come to rest for a period of time not exceeding thirty seconds. Next, the potentials are scanned in a positive (anodic) direction at a scan rate which usually does not exceed fifty millivolts per second. As the oxidation potential for the metal is approached, an increase in current occurs until a maximum value is reached, after which the current returns to the original value. At this point, the reduced form of the metal, through a charge-transfer reaction, has been oxidized or stripped off of the electrode. The result of the total process (shown in Figure 1) is a peak, the height of which is proportional to the concentration of the metal in solution.

E_{el} = pre-electrolysis potential
$E_{1/2}$ = half-wave potential
I_p = peak current
E_p = peak potential
I_L = limiting current
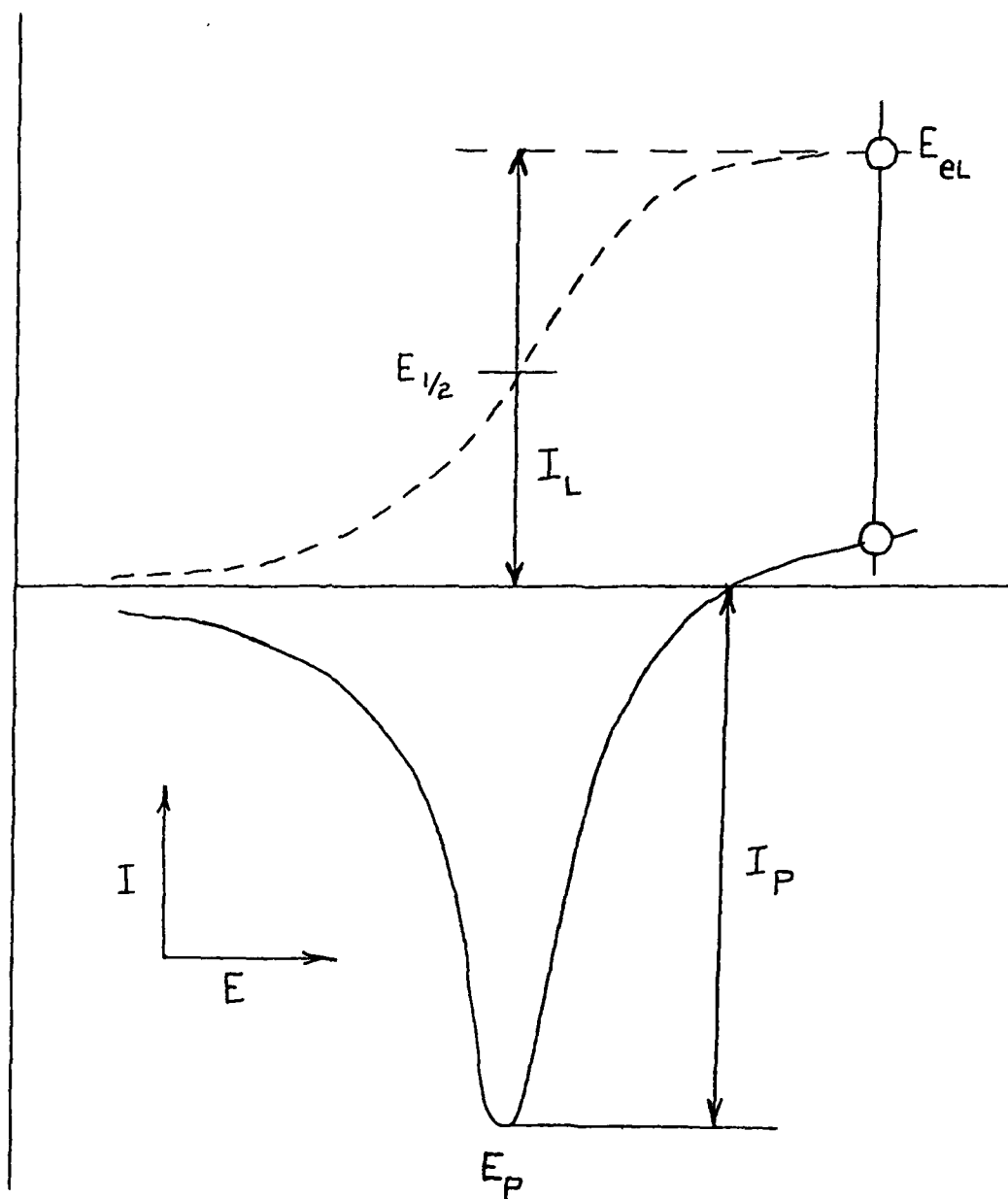
Figure 1.   The Analytical Features of an ASV Stripping
           Peak.

II. THEORETICAL ASPECTS OF ANODIC STRIPPING VOLTAMMETRY

A. Electrochemical Processes

As discussed earlier, a stripping determination involves the electrochemical deposition of some substance on an electrode followed by electrochemical dissolution of the deposit. In order to logically choose the conditions for a stripping determination and a priori ascertain the attainable sensitivity, it is imperative to be familiar with the basic electrochemical characteristics of the system under study. Therefore, prior to a discussion of the conditions for the formation of amalgams and films on electrodes and their subsequent dissolution, a discussion of the basic principles of electrode-process kinetics is necessary.

Electrochemical processes are generally very complex but can be schematically represented by three separate steps: (1) transport of the electroactive species to the electrode, (2) charge-transfer between the electrode and the electroactive species, and (3) transport of the charge-transfer reaction products away from the electrode. These three steps are carried out in solution in the presence of a sufficient excess of electrolyte. The electrolyte serves several purposes including maintaining electrical conductivity in the solution so that the IR drop is small, suppressing migration currents of the electroactive species, maintaining the activities of the electroactive components at constant values, and maintaining the structure of the electrical double-layer

so that changes in the electro-kinetic potential may be neglected.

Electrochemical processes are controlled by various internal processes, the rates of which determine the overall rate of the electrode process. The four major electrode processes are those which are controlled by (1) the rate of the charge-transfer reaction, (2) the rate of mass transport, (3) chemical reaction kinetics, and (4) deposit formation on the electrode. Of these four categories, only the first two will be considered. Chemical reaction kinetics controlled processes are quite complex and are usually avoided. Deposit formation concerns the use of solid electrodes, an area outside the scope of this work.

Electrode processes controlled by the rate of mass transport can be classified into stationary (steady-state) or non-stationary processes. The non-stationary process is theoretically useful to ASV and is treated in detail in section II-B.

In the steady state, a stationary distribution of the concentration of the electroactive species forms in the vicinity of the electrode, called the Nernst diffusion layer, δ_O (see Figure 2). Nernst[3] assumed that no convective electrolyte motion occurs within the diffusion layer, that the concentration gradient of the electroactive species is given solely by diffusion and that it is linear. From this assumption the concentration gradients can be expressed in terms of the cathodic reaction, where $C_{red}^o = 0$, by the
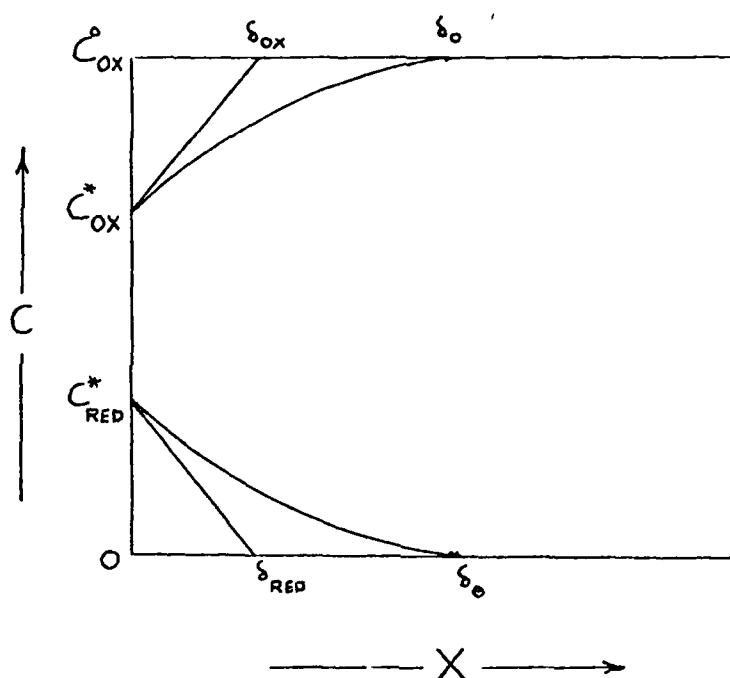
Figure 2. The Dependence of the Concentrations of the
Oxidized and Reduced Species on the Distance
from the Electrode Surface, X, for the reaction
Ox + ne $\longrightarrow$ Red in the Steady State

C^*_{ox}, C^*_{red} — Concentration at the Electrode
Surface

C^o_{ox}, C^o_{red} — Initial Concentrations in the Solution

δ_{ox}, δ_{red} — The Nernst Diffusion Layer Thickness
for ox and red, Respectively.

following equations:

$$\left(\frac{\partial C_{ox}}{\partial x}\right)_{x=0} = \frac{C^o_{ox}-C^*_{ox}}{\delta_{ox}} \; ; \quad \left(\frac{\partial C_{red}}{\partial x}\right)_{x=0} = \frac{-C^*_{red}}{\delta_{red}} \quad (II-1)$$

The current density, where A(area) = 1, is then given by

$$i = nFD\left(\frac{\partial C}{\partial x}\right)_{x=0} \quad (II-2)$$

and consequently is expressed by the equation

$$i = nFD_{ox}\left(\frac{C^o_{ox}-C^*_{ox}}{\delta_{ox}}\right) = -nFD_{red}\left(\frac{C^*_{red}}{\delta_{red}}\right) \quad (II-3)$$

For the limiting current density, $C^*_{ox} = 0$; therefore

$$i_L = \frac{nFD_{ox}C^o_{ox}}{\delta_{ox}} \quad (II-4)$$

where D is the diffusion coefficient of the indicated species. Equation (II-4) is a very important equation since it essentially describes the preconcentration process. The equation is quite general, but is only a good first approximation since it is based on the assumptions of zero convective movement and a linear concentration gradient within the diffusion layer which are not fulfilled in practice. Realistically, zero convective movement occurs only at the electrode surface and increases in a continuous manner perpendicular to the electrode and finally reaches a constant value at some distance from the electrode. This distance, the boundary layer, δ_0, is a hydrodynamic quantity which, assuming laminar flow is approximated by

$$\delta_O \simeq \left(\frac{\ell \nu}{U_O}\right)^{\frac{1}{2}} \qquad (II-5)$$

where

> ℓ is the appropriate electrode dimension
>
> ν is the kinematic viscosity defined by the ratio of the solution viscosity to the solution density
>
> U_O is the mean relative velocity of the solution with respect to the electrode suface.

The diffusion layer or boundary layer thickness can be determined for some practical systems. For example, a rotating electrode with entirely turbulent flow has been described.[4,5] The diffusion layer thickness is inversely proportional to the rotation speed of the electrode, ω.[6]

$$\delta = k/\omega$$

where k is a proportionality constant dependent on the electrode dimensions and the kinematic viscosity of the solution.

Now, it is important to consider the special case where the rate of mass transport is comparable to the rate of charge transfer since many ASV analyses occur under these conditions.[7] Therefore, the following equation (which is merely stated here and not derived) must be considered.

$$i = nFAk' \left\{ C_{ox}^* \exp\left[\frac{-\alpha nF}{RT}(E-E^{\circ\,\prime})\right] - C_{red}^* \exp\left[\frac{(1-\alpha)nF}{RT}(E-E^{\circ\,\prime})\right] \right\} \quad (II-7)$$

where:

> k' is the charge transfer rate constant
>
> $E^{\circ\,\prime}$ is the normal potential
>
> α is the charge transfer coefficient and the other symbols have their usual meanings.

Equation (II-7) is the polarization curve equation for electrochemical processes controlled by the rate of charge transfer. When equation (II-3) is substituted into equation (II-7), the resulting equation describes the special case mentioned above.

$$\frac{i_L-i}{i} \frac{x_{red}}{x_{ox}} = \exp\left[\frac{nF}{RT}(E-E^{\circ\,\prime})\right] + \frac{x_{red}}{nFk^{\prime}} \exp\left[\frac{\alpha nF}{RT}(E-E^{\circ\,\prime})\right] \qquad (II-8)$$

where: $x_{ox} = \dfrac{nFD_{ox}}{\delta_{ox}}$, and $x_{red} = \dfrac{nFD_{red}}{\delta_{red}}$

However, for reversible systems where $k^{\prime}$ is large, the second term on the right hand side of equation (II-8) may be neglected and, after rearrangement, equation (II-9) is obtained.

$$E=E^{\circ\,\prime}+ \frac{RT}{nF} \ln \frac{x_{red}}{x_{ox}} + \frac{RT}{nF} \ln \frac{i_L-i}{i} = E_{\frac{1}{2}} + \frac{RT}{nF} \ln \frac{i_L-i}{i} \qquad (II-9)$$

since by definition $E_{\frac{1}{2}} = E^{\circ\,\prime} + \dfrac{RT}{nF} \ln \dfrac{x_{red}}{x_{ox}}$

Equation (II-9) is the well-known equation of a reversible cathodic voltammetric (polarographic) wave with half-wave potential $E_{\frac{1}{2}}$.

If, however, the system behaves irreversibly, and $k^{\prime}$ is very small, the first term on the right-hand side of equation (II-8) may be neglected, yielding

$$E=E^{\circ\,\prime} + \frac{RT}{\alpha nF} \ln\frac{nFk^{\prime}}{x_{ox}} + \frac{RT}{\alpha nF} \ln \frac{i_L-i}{i} =$$

$$(E_{\frac{1}{2}}cath)_{irr} + \frac{RT}{\alpha nF} \ln \frac{i_L-i}{i} \qquad (II-10)$$

The equations (II-9 and II-10) derived above work well for stationary or steady-state conditions. If, however, the electrode process occurs under non-stationary conditions, the concentration of the electroactive species becomes a function of time. The description of such a process must involve the solution of Fick's Law of Diffusion (Second Law) equation. The equation is usually formulated in terms of both soluble oxidation forms C_{ox} and C_{red}:

$$\frac{\partial C_{ox}}{\partial t} = D_{ox}\left(\frac{\partial^2 C_{ox}}{\partial x^2}\right) \quad \frac{\partial C_{red}}{\partial t} = D_{red}\left(\frac{\partial^2 C_{red}}{\partial x^2}\right) \qquad \text{(II-11)}$$

along with the following initial and boundary conditions.

(1) The initial concentrations are constant in the solution

$$x > 0, \ t = 0; \ C_{ox} = C_{ox}^o, \ C_{red} = 0$$

(2) Diffusion flux at the surface of the electrode is related to the rate of the charge transfer reaction.

$$x = 0, \ t > 0; \ D_{ox}\left(\frac{\partial C_{ox}}{\partial x}\right) = -D_{red}\left(\frac{\partial C_{red}}{\partial x}\right) =$$

$$k'\{\exp\left[\frac{-\alpha nF}{RT}(E-E^{o\prime})\right]C_{ox} - \exp\left[\frac{(1-\alpha)nF}{RT}(E-E^{o\prime})\right]C_{red}\}$$

(3) At a large distance from the electrode, the system remains unchanged.

Solutions of equation (II-11) are of the utmost importance for the electrochemical dissolution of deposits from an electrode. Solutions have been obtained for various electrodes. Since this research was conducted with the hanging mercury drop electrode, the solution to equation (II-11) will

be described for the special case of metals stripped from a
stationary mercury drop electrode.

B. Mathematical Treatment of the Spherical Mercury Drop
    Electrode

To apply equation (II-11) to stripping determinations of
metals at the mercury drop electrode, it must be remembered
that the reduced species concentration must be replaced by
the metal concentration. Also, the mercury drop electrode
has a finite volume which will lead to deviations not predict-
ed by the treatment expounded in the previous section, which
assumed semi-infinite linear diffusion.

Reinmuth[8] developed a theoretical description of
stripping voltammetry with spherical electrodes and hypo-
thetically divided the deviations from semi-infinite linear
diffusion into two causes. One of which is the curvature of
the electrode and the other is the finite volume of the elec-
trode. The electrochemical behavior at a planar mercury
electrode having finite thickness is developed first to
illustrate the differences between the spherical and planar
treatments.

Reinmuth assumed linear metal diffusion in the planar
mercury electrode and formulated the following initial and
boundary conditions:

(1) $t = 0$, $0 < x < \ell$; $C_R = C_R^*$

(2) $t > 0$, $x = 0$; $D_R(\partial C_R / \partial x) = 0$

(3) $t > 0$, $x = \ell$; $C_R = f$

where:

t is time

x is the linear distance

ℓ is the electrode thickness

C_R^* is the homogeneous initial concentration of
the reduced form within the electrode

D_R is the reduced form's diffusion coefficient

The first condition explains the initial situation prior
to pre-electrolysis. The second condition indicates that
no material enters or leaves the back side of the electrode.
The third condition defines the concentration of R at the
electrode-solution interface in terms of a function f which
is in turn related to the charge transfer reaction described
by equation (II-7) in the previous section. By Laplace trans-
formation of the Fick equation and substitution of conditions
1 to 3, the Laplace transform of the current at the electrode-
solution interface is of the form

$$\bar{I}_o = nF\ (\bar{f} - C_R^*/S)\ \sqrt{SD}\ \tanh(\ell\sqrt{S/D}) \tag{II-12}$$

where:

S is the transform variable

$\bar{I}_o$ is the transform of the current density

$\bar{f}$ is the transform of the function f which must be
known in order that the inverse transformation
of equation (II-12) be carried out and an explicit
relation for the current obtained.

At a spherical electrode, a different form of the Fick
equation is used and the boundary conditions are rewritten
as follows:

(4) $t=0$, $0 < r < r_0$; $C_R = C_R^*$

(5) $t > 0$, $r \longrightarrow 0$; C_R remains bounded

(6) $t > 0$, $r = r_0$; $C_R = f$

where:

r_0 is the radius of the electrode

r is the spherical coordinate

The analog of condition 2 is modified because of the change in area of the system with respect to radial distance in a spherical system. By substitution of conditions 4 to 6 and transformation, a similar relation for a spherical electrode is obtained.

$$\bar{I}_0 = nF(\bar{f} - C_R^*/S)\sqrt{SD}\coth(r_0\sqrt{S/D}) - nfD(\bar{f} - C_R^*/S)r_0 \qquad (II-13)$$

In comparing equations (II-12) and II-13), the tanh term is replaced by coth and a correction term for spherical diffusion, $-nfD(\bar{f} - C_R^*/S)/r_0$, is added. The hyperbolic factor, coth, can be thought of as taking account of the finite electrode size of the spherical drop. For large ℓ and r_0 values, equations (II-12) and (II-13) are converted into equations for semi-infinite diffusion. (i.e. the hyperbolic terms become equal to unity and the last term in equation (II-13) approaches zero in the limit.). Assuming that the electrode reaction is reversible and $D_R = D_0$, where D is the diffusion coefficients, both forms being soluble in solution or in the electrode, we can write

$$C_R + C_0 = C_0^* + C_R^* \text{ at } r = r_0 \qquad (II-14)$$

From this relation, the function f can be calculated using the Nernst equation.[9]

Shain and Levinson[10] have shown that under normal
conditions of stripping analysis with stationary drop elec-
trodes, only the spherical correction need be considered and
the limited volume correction can be neglected. Curves cal-
culated from equations derived from this assumption agree
well with experimental voltammagrams as shown in Figure 3.

C. Amalgam Properties

During the pre-electrolysis step of a stripping determi-
nation involving the use of a mercury electrode, the metal is
deposited within the mercury and forms a metal amalgam. There-
fore, a basic understanding of the interactions of metals with
mercury is necessary.

The properties that are of particular interest in
stripping analysis with the HMDE are: (1) the solubility in
mercury of the metals to be determined, (2) the possibility
of formation of intermetallic compounds, and (3) the electro-
chemical properties of amalgams.

A large research effort has been conducted on determin-
ing the solubilities of many metals in mercury, the values
of which are shown in Table 1. The solubilities are quite
temperature dependent, especially for Zn, Cd, Sn, Pb, and the
metals of the gallium group. Although attempts have been made
to quantify and characterize solubility according to atomic
number, no general law has been found.[11]

As mentioned previously, when several metals are present
simultaneously in mercury, intermetallic compounds between
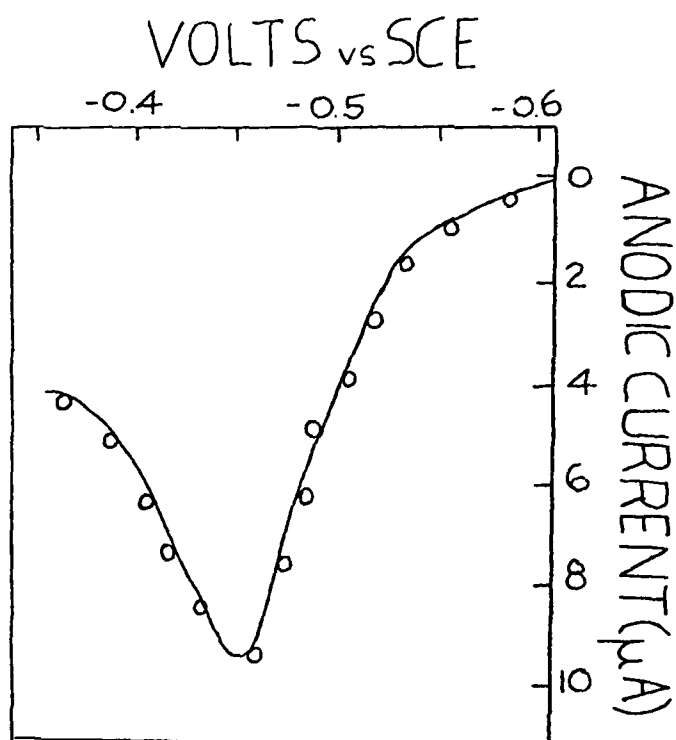the dissolved metals are frequently formed. Generally, metals

Figure 3.   Current-voltage Curve for Anodic Stripping
            of Thallium, using Voltammetry with linearly
            Varying Potential.[10]

            —— Experimental
            ooo Theoretical

TABLE 1

SOLUBILITY OF METALS IN MERCURY[11]

METAL	TEMPERA-TURE °C	SOLUBILITY		METAL	TEMPERA-TURE °C	SOLUBILITY	
		% w/w	atom %			% w/w	atom
Li	25	0.048	1.34	Pu	20	0.0154	0.0127
Na	25	0.57	4.8	Si	20	(0.001)	0.007
K	25	0.395	2.0	Ge	25	1×10^{-6}	--
Rb	25	1.37	3.15	Sn	20	0.6	1.26
Cs	25	4.0	6.0	Pb	20	1.1	1.1
Cu	20	0.003	0.006	Ti	20	5×10^{-6}	2×10^{-5}
Ag	20	0.035	0.066	Zr	20	0.003	0.007
Au	20	0.1306	0.1329	Sb	20	2.9×10^{-5}	4.7×10^{-5}
Be	100	10^{-6}	2×10^{-5}	Bi	20	1.1	1.1
Mg	17	0.31	2.5	V	20	5×10^{-5}	2×10^{-4}
Ca	25	0.30	1.48	Nb	20	(0.001)	0.002
Sr	20	1.04	2.34	Cr	20	3.1×10^{-11} to 4×10^{-7}	--
Ba	20	0.33	0.48	Mo	20	2×10^{-5}	4×10^{-5}
Zn	20	1.99	6.4	W	20	10^{-5}	10^{-5}
Al	20	0.002	0.015	Fe	20	1.15×10^{-17} to 7×10^{-5}	--
Ga	22	1.13	3.19	Co	20	8×10^{-5}	--
In	20	57	70.3	Ni	20	4.8×10^{-5}	--
Tl	20	42.8	42.6	Ru	20	0.353	0.694
La	25	0.0092	0.0133	Rh	20	0.16	0.311
Ce	20	0.016	--	Pd	20	0.006	0.012
Th	20	0.016	0.014	Ir	20	0.001	0.001
U	20	0.005	0.0042	Pt	24	0.09	0.10

which do not normally form solid alloys (e.g. Bi-Sn, Cr-Sn, and Bi-Pb) do not mutually react in mercury, either. However, the existence of a normal solid alloy does not insure the corresponding reaction in mercury (e.g. solid alloys formed by the metallic couples Sb-Sn, Ag-In, and Ni-In do not form intermetallic compounds in mercury). Interaction of metals in mercury is usually extremely low if the metals are sparingly soluble in mercury to begin with (e.g. compounds of the type Fe-Cr, and Co-Cr are not formed at all).[11] The introduction of a more noble metal into the mercury may bring about intermetallic compound formation with the metal(s) already present (e.g. Zn-Au, Cd-Au, Zn-Cu, Sn - Cu, Co-Zn, and Zn-Ni). The solubility products of some intermetallic compounds in mercury are listed in Table 2.

The electrochemical properties of amalgams have been rigorously described by several researchers[12,13] and have generally centered on describing the equilibrium potential of a single-phase amalgam where the concentration cell consists of the pure metal and it's saturated amalgam immersed in a solution of a salt of the metal. The values of the charge-transfer rate constants and coefficients for several amalgam electrodes are given in Table 3.

An illustrative case of the electrochemical behaviour (as applied to ASV) of an amalgam containing an intermetallic compound is found in the study of the Ni-Zn[17,18] system. The intermetallic compound forms at concentrations of Ni higher than 10^{-5}M. (See Figure 4). First, only the peak

TABLE 2

THE SOLUBILITY PRODUCT VALUES FOR SOME INTERMETALLIC

COMPOUNDS IN MERCURY AT $20°C$[11]

COMPOUND	SOLUBILITY PRODUCT	COMPOUND	SOLUBILITY PRODUCT
AuZn	2.5×10^{-12}	CuGa	2×10^{-6}
AuCd	2.5×10^{-9}	CuSb	3.2×10^{-7}
AuIn	1.8×10^{-6}	SbZn	2×10^{-9}
AgZn	3×10^{-6}	SbCd	1×10^{-8}
AgCd	7×10^{-6}	SbIn	2×10^{-8}
CuZn	4×10^{-6}	$MnCd_3$	5.7×10^{-11}
Cu_3Sn	3×10^{-12}	$MnSn_2$	7×10^{-9}
CuSn	4×10^{-7}	GaCo	2.6×10^{-16}
$CuGe_3$	8.4×10^{-13}	GaNi	3.9×10^{-16}

TABLE 3

THE k' AND α VALUES FOR SOME AMALGAM ELECTRODES

REACTION	BASE ELECTROLYTE	k'(cm/s)	α	REF.
$Bi^{3+} + 3e = Bi(Hg)$	1 M $HClO_4$	3×10^{-4}	--	14
$Cd^{2+} + 2e = Cd(Hg)$	1 M KNO_3	0.6	--	14
$Cu^{2+} + 2e = Cu(Hg)$	1 M KNO_3	4.5×10^{-2}	--	14
$Zn^{2+} + 2e = Zn(Hg)$	1 M KCl	4×10^{-3}	--	14
		--	0.15	15
$Pb^{2+} + 2e = Pb(Hg)$	1 M KCl(pH 2)	0.2	0.94	15
$Tl^{+} + e = Tl(Hg)$	1 M KNO_3(pH 2)	0.3	0.8	15
$Zn^{2+} + 2e = Zn(Hg)$	1 M KCl	4×10^{-3}	0.36	16

+2.0V   0.0V   -1.4V

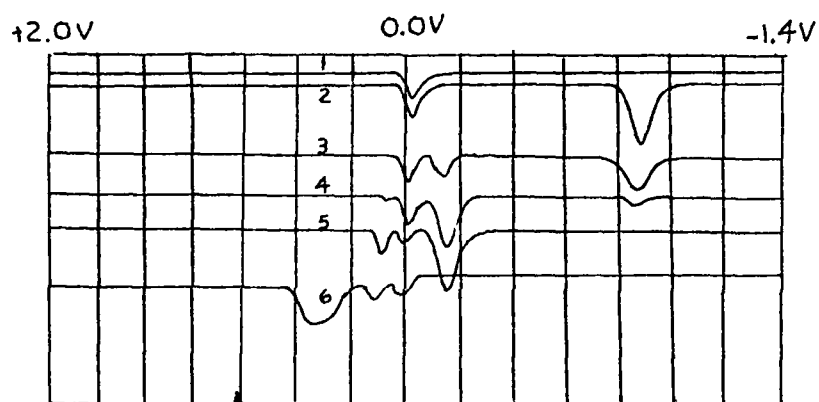Figure 4.   The Polarization Curves of Oxidation of
the Zinc-Nickel Amalgam

T = 2 min, E_{el} = -1.4V; (1)base electrolyte, 0.1M KCl; (2)5×10^{-4}N Zn^{2+}; (3)5×10^{-4}N Zn^{2+}+2×10^{-4}N Ni^{2+}; (4)5×10^{-4}N Zn^{2+}+4×10^{-4}N Ni^{2+}; (5)5×10^{-4}N Zn^{2+} + 6×10^{-4}N Ni^{2+}; (6)2×10^{-4}N Ni^{2+}.

corresponding to Zn oxidation is observed on the amalgam
oxidation polarization curve; with increasing Ni concentration,
the Zn peak becomes smaller and a more positive peak corre-
sponding to the oxidation of the intermetallic compound
appears. Finally, at higher Ni concentrations, the Zn peak
completely disappears and only the oxidation peaks of the
intermetallic compound and Ni are present.

D. The Electrochemistry of Chromium

Chromium forms compounds having the oxidation states
+2, +3 and +6. The +2 state is basic with the chromous ion
being a powerful reducing agent that is not stable in aqueous
solutions even at low hydrogen ion concentrations. The +3
state is amphoteric, forming compounds of the chromic ion
with acids and chromites with bases. Chromium trioxide,
CrO_3, is soluble in water. One of the principal character-
istics of the trioxides of chromium is the formation of
oxyanions such as the chromate ion, CrO_4^{2-}, and the dichromate
ion, $Cr_2O_7^{2-}$.

In a number of electrolytes, both chromium(III) and
chromium(VI) are reduced to the metal, which is sparingly
soluble in mercury (see Table 1). In addition, there are a
number of electrochemical reactions involving the following
oxidation state changes: $Cr(VI) \rightleftharpoons Cr(III) \rightleftharpoons Cr(II)$. The
half-wave potentials for several chromium complexes are given
in Table 4, along with the medium used and the oxidation
states involved. Dichromate is reduced to chromium(III) in
H_2SO_4 more concentrated than 0.1 M at approximately 0V; in

TABLE 4

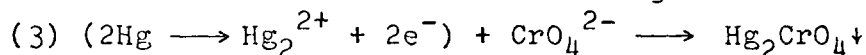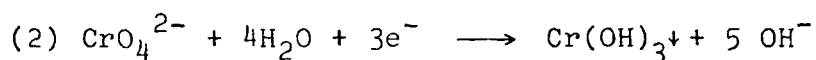### Half-Wave Potentials of Chromium Complexes[19]

Complex	Medium	Reaction	$E_{1/2}$
$Cr_2O_7^{2-}$	H_2SO_4	6 ⟶ 3	↑*
	KCl	6 ⟶ 3	−0.28 −0.96
		3 ⟶ 2	−1.50
		2 ⟶ 0	−1.70
	KOH	6 ⟶ 3	−1.03
	0.1M NH_3, 0.1M NH_4Cl	6 ⟶ 3	−0.46
$Cr(H_2O)_6^{3+}$	K_2SO_4	3 ⟶ 2	−1.03
		2 ⟶ 0	−1.63
$CrCl_6^{3-}$	10M $CaCl_2$	3 ⟶ 2	−0.51
$Cr(NH_3)_X^{3+}$	NH_3, NH_4Cl	3 ⟶ 2	−1.42
	0.005% gelatin		
$Cr(Py)_X^{3+}$	0.1M Py, 0.1M Py·HCl	3 ⟶ 2	−0.95
$Cr(CN)_6^{3-}$	KCN	3 ⟶ 2	−1.38
Cr^{2+}	0.1M Na_2SO_4	2 ⟶ 3	−0.58
$Cr(NH_3)_X^{2+}$	5M NH_4Cl, 0.1M NH_3	2 ⟶ 3	−0.30

* The reduction of the complex starts from zero applied voltage.

less acidic solutions, $Cr(OH)_3$, is formed on the electrode surface. Also, in a neutral solution, such as 0.1 M KCl, dichromate gives several reduction waves corresponding to +6 to +3, +3 to +2, and +2 to 0.

For pre-electrolysis in striping determinations, almost all the reactions made possible by the various oxidation states of the metal have been employed, namely:

(1) $Cr^{3+} + 3e^- \longrightarrow Cr(Hg)$

(2) $CrO_4^{2-} + 4H_2O + 3e^- \longrightarrow Cr(OH)_3\downarrow + 5\ OH^-$

(3) $(2Hg \longrightarrow Hg_2^{2+} + 2e^-) + CrO_4^{2-} \longrightarrow Hg_2CrO_4\downarrow$
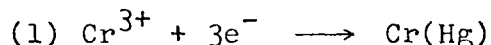
Reaction (1) has not yielded very satisfactory analytical results. By pre-electrolysis at $E_{el} = -1.2V$ from 1 M Na_2HPO_4 and exchange of the solution for 0.1 M KSCN, a stripping peak is obtained at -0.85 V.[20] The drawback of this technique is the acute non-linearity of the calibration curve.

Reaction (2) seems to be the most promising. Inert electrodes, especially graphite ones, are suitable. The results of the study of this reaction with a wax impregnated graphite electrode (WIGE) in a number of electrolytes are shown in Table 5. The values of Ep_{cath} are given for the sake of comparison since the cathodic peaks are as much as 1.0 V more positive than the anodic ones, owing to the irreversibility of chromate reduction.

Reaction (3) is also a useful method but in a cathodic stripping voltammetric (CSV) method and is therefore limited to the detection of anionic species.

TABLE 5

Stripping Voltammetric Determination of Chromium

in the Form of $Cr(OH)_3$ [21]

Base Electrolyte	pH	$E_{\frac{1}{2}}$	E_{el}	E_p	C_{min}, M
0.05M $Na_2B_4O_7$	9.5	−0.70	−1.0	+0.6	2×10^{-7}
$C_3H_4(OH)(COOH)_3$ + NaOH	5.2	−0.35	−0.5	+0.7	1×10^{-6}
KH_2PO_4 + NaOH	8.0	−0.35	−0.7	+0.07	1×10^{-7}
0.4M NH_4Cl + 0.1M NH_4OH		−0.45	−0.7	+0.6	4×10^{-8}
0.1M CH_3COOH + 0.1M CH_3COONa		−0.10	−0.5	+0.9	2×10^{-6}
0.01M H_2SO_4		+0.20	+0.3	−0.6	1×10^{-5}

E_{el} – pre-electrolysis potential

E_p – cathodic stripping peak potential

C_{min} – minimum concentration determinable

E. The ASV Analysis of Chromium using the Hanging Mercury
    Drop Electrode: Outline of Research

As seen in the previous section, several methods are
available for the stripping determination of chromium. How-
ever, no satisfactory method has been developed which employs
the hanging mercury drop electrode. The need for developing
such a method arises for several reasons. First of all, the
HMDE is an extremely versatile and convenient electrode used
in the determination of a wide range of metals and non-metals.
Secondly, chromium analysis is of the utmost importance in
environmental and bio-medical fields. Finally, any method
which can add chromium to the battery of elements which can
be determined by the HMDE will increase the analytical chemists'
ability to perform routine analyses of systems containing
multiple elements and, thereby, allow the analyst to make a
more accurate assessment of the analytical problem he is
facing.

Therefore, this research centered on developing an ASV
technique using the HMDE which could detect concentrations of
chromium on the order of a part per million. The research was
a three-prong attack of the problem consisting of investi-
gations into the effect of ionic strength on peak current;
an attempt to increase technique sensitivity by polymeric film
formation; and the use of the CrO_4^{2-}/NaOAc system in the
actual analysis of chromium.

III. EXPERIMENTAL

A. Reagents and Equipment

The reagents used in this research were Baker reagent grade KNO_3, sodium acetate and ammonium acetate both of which were Fisher certified reagent grade, and dithiodiglycolic acid (carboxymethyl disulphide) from the Aldrich Chemical Company. A primary standard of 99.7% pure $K_2Cr_2O_7$ was used in the synthesis of chromium(III).[22] Harleco atomic absorption standards (1000 ppm) were used as stock solutions to prepare standards of CrO_4^{2-}, Zn, Pb, and Cd.

All glassware was thoroughly washed, rinsed with DI H_2O and soaked in a 1% EDTA solution overnight. Between runs, the glassware was rinsed immediately with 1% EDTA and DI water. In addition, the 250 ml, wide-mouth plastic bottles used to store standards were leached for 24 hours in 1% EDTA solution. Without this leaching process, significant levels of zinc were detected during analyses. Glass vessels did not present this problem; therefore, glass containers instead of plastic ones should be used in further research of this nature.

Electronic equipment used in the research consisted of the voltammetry unit, Model CV-1A from Bioanalytical Systems, connected to an Omnigraphic Model 2122-6-5 recorder from the Houston Instrument Company.

The electrolytic cell was a jacketed titration vessel from Brinkman Instruments, Inc., and was connected via 1/4

28

inch, thick-walled vacuum tubing to a Haake-F-junior (FJ and FE) constant temperature circulation pump. The electrodes used were a saturated calomel electrode, Metrohm EA404, and a hanging mercury drop electrode (see Figure 5), Metrohm E-410, from Brinkman Instruments, Inc. Completing the three-electrode arrangement, a platinum wire was used as the auxiliary electrode. Also, an in-house fabricated dropping mercury electrode (DME) arrangement was used in a polar-graphic study of chromium.

B. The Hanging Mercury Drop Electrode

The hanging mercury drop electrode served as the working electrode throughout this research, except in the polaro-graphic study where the dropping mercury electrode was used. The HMDE is a convenient and precise electrode due to its capability of replenishing the electrode surface consistently and accurately throughout an ASV determination. After a run, a new drop can be formed at the capillary orifice by turning the microfeeder knob through a desired number of scale divisions. The exact drop sizes for certain scale divisions of the Metrohm E-410 HMDE have been determined by optical methods and are shown in Table 6.[23]
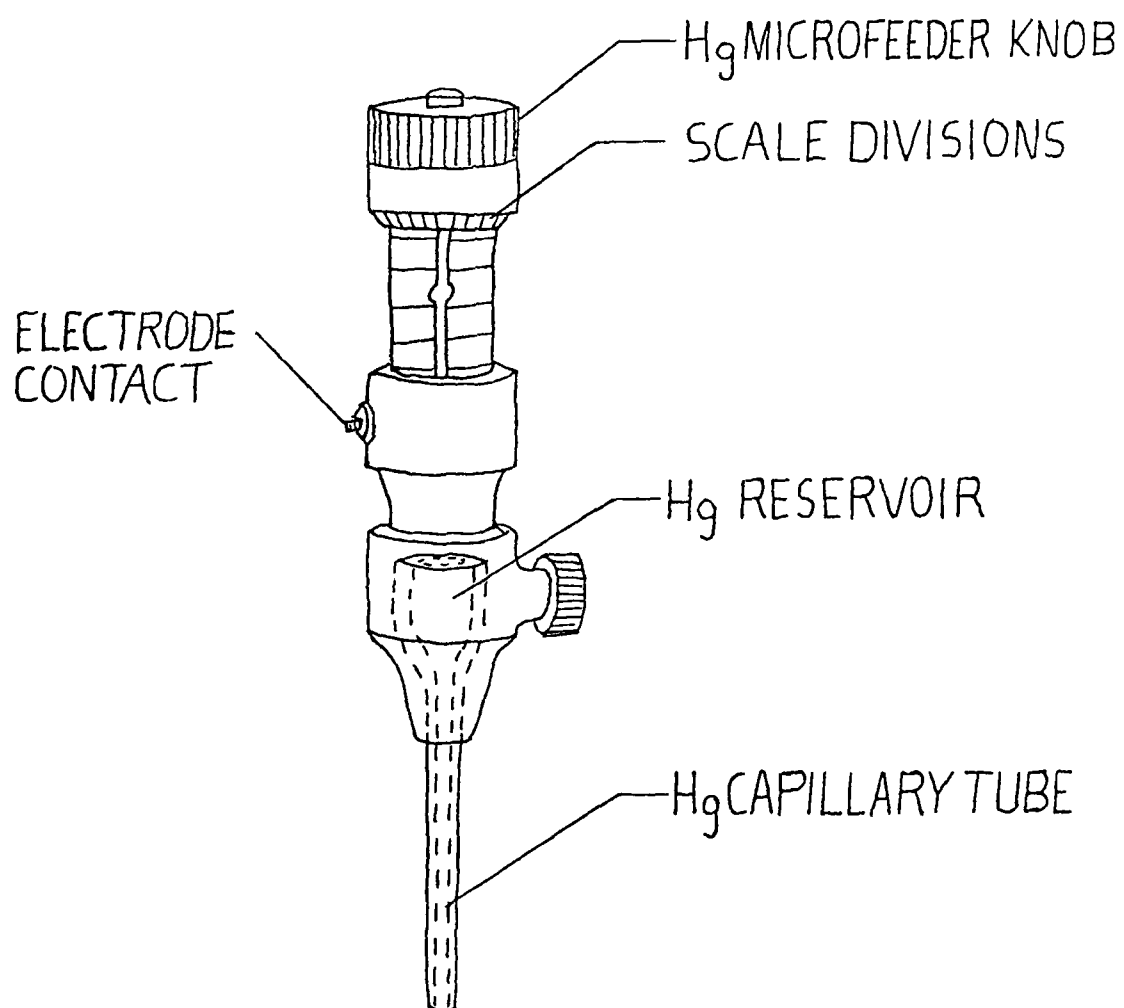
Figure 5.   Diagram of the Hanging Mercury Drop Electrode

TABLE 6

Drop Sizes of the E-410 HMDE

Scale Divisions on E-410	Drop Diameter in mm	Drop Surface Area in mm^2
1	0.52	0.86 ± 0.03
2	0.66	1.38 ± 0.04
3	0.76	1.80 ± 0.05
4	0.83	2.22 ± 0.07

IV. RESULTS AND DISCUSSION

A. The Effects of Ionic Strength on Stripping Peak Current

   for the Chromium(III)/KNO$_3$ System

   As a starting point for this research, the effects of
ionic strength on stripping peak current were studied. The
investigation was to determine an optimum ionic strength
that would give sensitive and reproducible results. Also,
this portion of the research was very repetitive and there-
fore ideally suited to "hands-on" training with the rather
complicated electronic equipment that was involved.

   Generally, the height of a measured voltammetric peak
decreases with increasing salt concentration;[24] however,
such a generality is of little use for specific systems
and optimization of sensitivity and reproducibility must
be done experimentally.

   The molar ionic strength, μ_c, of a solution is expressed
as the following summation:

$$\mu_c = \tfrac{1}{2}\sum_i C_i Z_i^2 \qquad\qquad \text{(IV-1)}$$

where:

   C_i is the molar concentration of the ith ion
     expressed in moles per liter

   Z_i is the numerical charge of the ion.

For a simple one-to-one electrolyte such as KNO$_3$, the ratio
of the molarity to the ionic strength is unity and ionic
strength can be expressed simply as molar concentrations.

32

Four solutions containing concentrations of KNO_3 varying from 0.01 to 0.5 M were prepared. Twenty milliliter quantities of these solutions were transferred to the electrolytic cell. Sequential runs were made by delivering 200 µl amounts of 100 ppm chromium(III) standard into the cell with Eppendorf pipets, pre-electrolyzing at 1.4 V versus the SCE for five minutes while stirring the solution, then scanning the potentials anodically from -1.4 V to 0 volts. During these runs the temperature was thermostated at 22° ± 0.01°C. A series of ten runs were made at each of the four ionic strengths. An example of a typical working curve is shown in Figure 6 along with the indicated correlation factor and the slope of the least squares fit straight line in microamps per ppm.

Next, the slope values were plotted versus the ionic strength values. The plot, shown in Figure 7, indicates that as the ionic strength increases, the peak current decreases, and hence the overall sensitivity of the technique decreases. Also, at ionic strengths less than 0.1 M, reproducibility of data becomes a problem although peak current increases somewhat. By the same token, ionic strengths above 0.1 M gave good reproducibility but sensitivity decreased. Thus, the electrolyte concentration of 0.1 M appears to be the optimum ionic strength.

The behavior of peak current with ionic strength can also be rationalized from the "physics" of the system. For instance, the ionic strength effect on peak current must be due largely to the increasing viscosity of the solution,
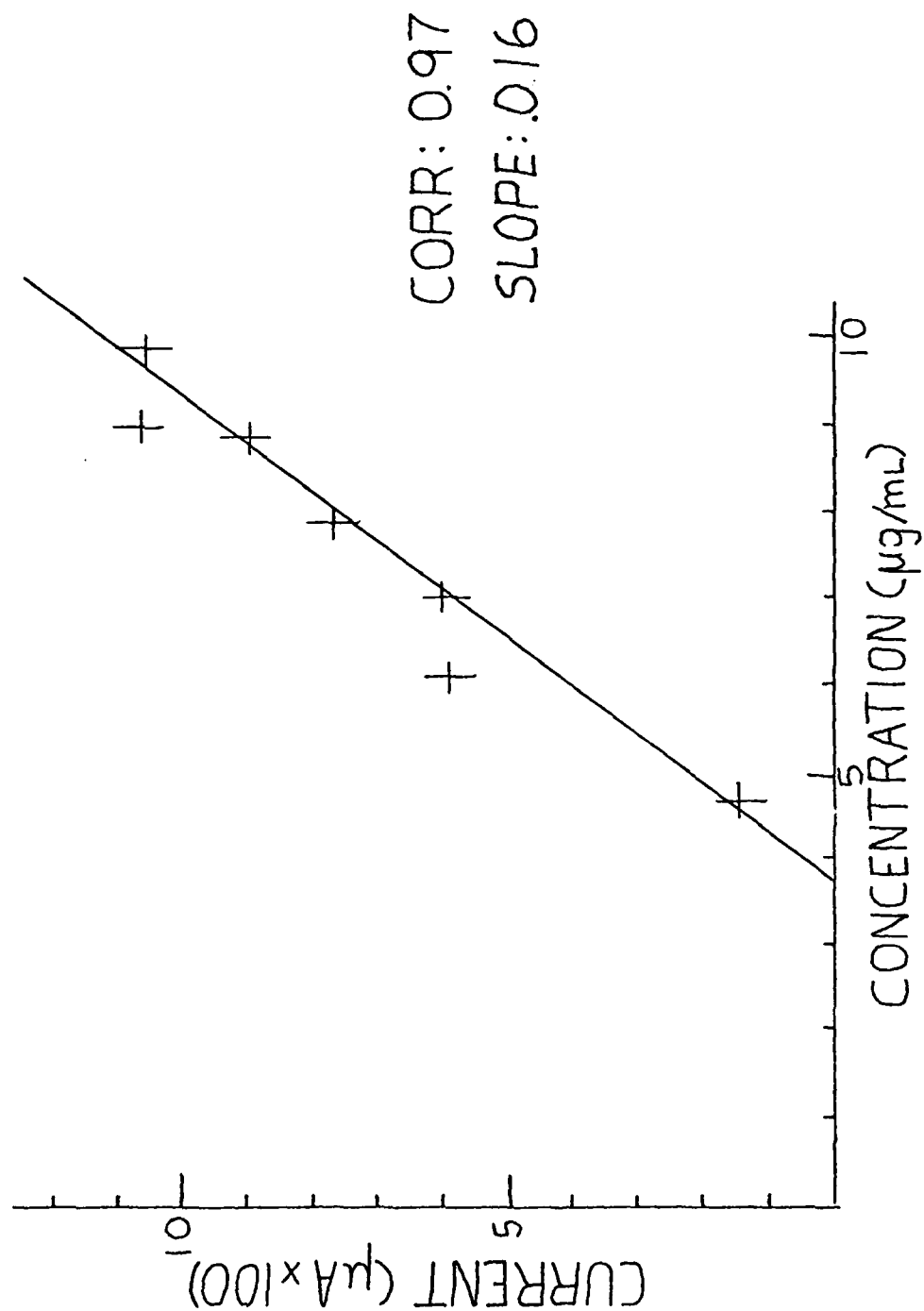
Figure 6. Peak Current versus Concentration of Chromium(III) in
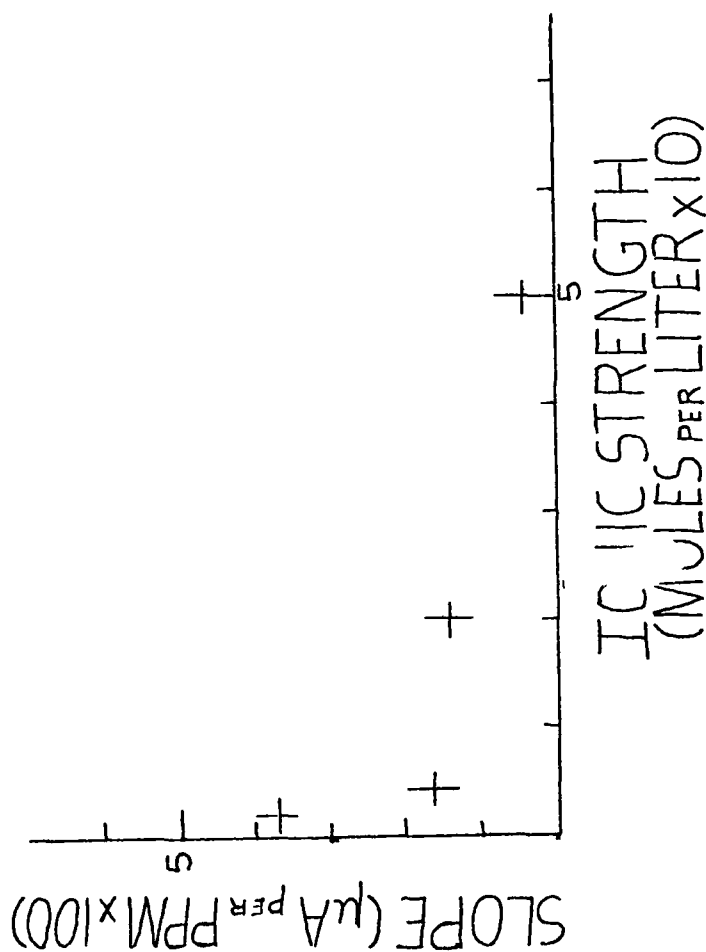0.05 F Potassium Nitrate

Figure 7. Calibration Curve Slope Values versus Ionic
Strength for Chromium(III) in Potassium Nitrate

which causes a proportional decrease in the rate of diffusion according to the Stokes-Einstein equation

$$D = kT/6\pi a\eta \tag{IV-2}$$

where

D is the rate of diffusion of the depolarizer

k is the Boltzmann constant

T is temperature in $°K$

a is the radius of a spherical particle

η is the viscosity of the solution.

Now, a relation between D and I_p must be found such that $I_p \propto D$. The limiting current flowing during the pre-electrolytic step is given by equation (II-4)

$$i_L = nFD_{ox}C^o_{ox}/\delta_{ox}$$

where all of the symbols have been previously defined. Using Faraday's Law, a relationship between the limiting current, i_L, and the concentration of the reduced metal in mercury, C_{Hg}, can be found such that

$$C_{Hg} = 3i_L T/4\pi r_o^3 nF \tag{IV-3}$$

where

T is the pre-electrolysis time in seconds

r_o is the radius of the mercury drop

Further, it is assumed that I_p is proportional to C_{Hg} and η is proportional to the concentration of the electrolyte (ionic strength). Given these assumptions and equations (IV-2) and (IV-3), the result is

$$I_p \propto 1/C_{electrolyte}$$

where $C_{electrolyte}$ is the electrolyte concentration or ionic strength.

The results of this investigation substantiate the assumption that peak current is decreased by increasing salt concentration and that 0.1 M is the salt concentration of choice for the chromium(III)/KNO_3 system. However, the overall sensitivity of this analysis is very poor (e.g., 0.016 μA/ppm for μ_c = 0.05 M), and the investigation into polymeric film formation was an attempt to achieve greater sensitivity.

B. Polymeric Film Formation: An Attempt to Achieve Greater Sensitivity

In the previous section, the sensitivity or signal-to-analyte ratio of chromium(III) in KNO_3 was very low. The low sensitivity must be due, in part, to the low solubility of chromium in mercury as indicated in Table 1. Therefore, any attempt to increase sensitivity must somehow circumvent the solubility problem. Such an attempt was made by investigating the effect of polymeric film on stripping peak current for chromium(III) and lead(II) was used as a model for comparison.

The adsorption on mercury of the complexes of several chelating carboxylate ligands bearing thioether groups with lead(II) and some other d^{10} metal cations was examined by Parkinson and Anson.[25] The extraordinarily large adsorption observed with a number of complexes was attributed to the formation of new phases on the mercury electrode surface. The structure of the absorbed films was thought to resemble the polymeric crystals formed by several metal salts of the same ligands. One of the structures which can be constructed

from molecular models appears in Figure 8.

Although Anson's work was with d^{10} metal cations, the possibility that other cations, such as chromium, may exhibit similar behavior was not discounted although the degree of adsorption varied markedly even among the d^{10} metal cations. Therefore, if chromium could form a polymeric film with a thioether containing ligand, then the film could be stripped *from the mercury electrode* while the peak current is monitored in the usual fashion. Since the model in Figure 8 suggests the existence of layer formation, it stands to reason that a considerable quantity of chromium could be deposited, accompanied by a commensurate increase in peak current.

The thioether ligand chosen for this research was dithiodiglycolic acid, $S_2(CH_2CO_2H)_2$. The di-sodium salt of the acid was prepared by adding 7.5 ml of 50% NaOH (0.2 moles) to 18.2 g. of $S_2(CH_2CO_2H)_2$(0.1 moles) according to the following equation:

$$S_2(CH_2CO_2H)_2 + 2NaOH \longrightarrow S_2(CH_2CO_2Na)_2 + 2H_2O$$
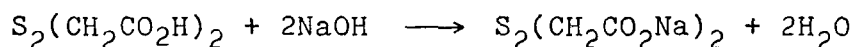
The resulting salt was recrystallized three times from a 1:1 water-ethanol solution. IR spectra of the disodium salt and the parent acid as KBR pellets were obtained. Upon conversion to the di-salt, the O-H stretching band of the di-carboxylic acid disappeared. Also, the broad, moderately strong absorption peak at approximately 900 cm^{-1} corresponding to the O-H bending frequency is absent in the IR spectrum of the disodium salt.
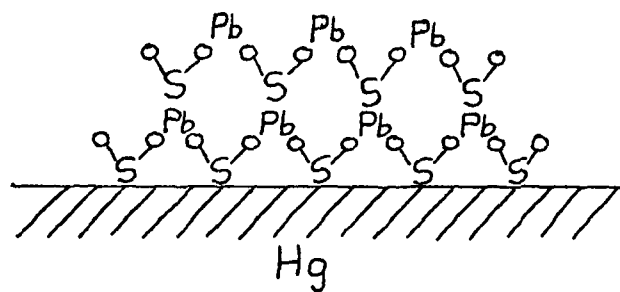
Figure 8.   Structure of the Polymeric Film of a Lead(II)-
Thioether Complex Absorbed on a Mercury
Electrode

The experimental technique involved making up solutions of 0.001 M dithiodiglycolate in which the electrolyte was 0.1 F NaOAc. The choice of sodium acetate instead of potassium nitrate was made because stripping peaks of chromium(III) in sodium acetate were larger and more well-defined than for the same concentrations of chromium(III) in potassium nitrate. (See Figure 9)

After the solutions were prepared, 20 ml portions were transferred to the electrolytic vessel, and a series of runs were made by adding 200 and 100 µl amounts of the metals to the solution containing the electrolyte and dithiodiglycolate. The experimental conditions for the runs were pre-electrolysis time, 5 minutes, the still time was 30 seconds, temperature kept constant at 22 ± 0.1°C, and scan rate was 50 mv/sec.

In the case of chromium(III), no significant increases in peak current were noticed in comparison with similar runs made in the same electrolyte without the presence of the dithio-diglycolate ligand. Evidently, chromium did not form a polymeric film as was hoped. Although no data was found, it may be that chromium(III) is not strongly chelated by the dithiodiglycolate ligand even though it has four "hard" oxygen donor atoms which should interact with the "hard" chromium(III) cation.

However, as shown in Figure 10, at a lead(II) concentration of 2.5 µg/ml a large increase in current was measured. Unfortunately, the increase in current was non-linear and extremely unpredictable. Thus, lead is probably forming the
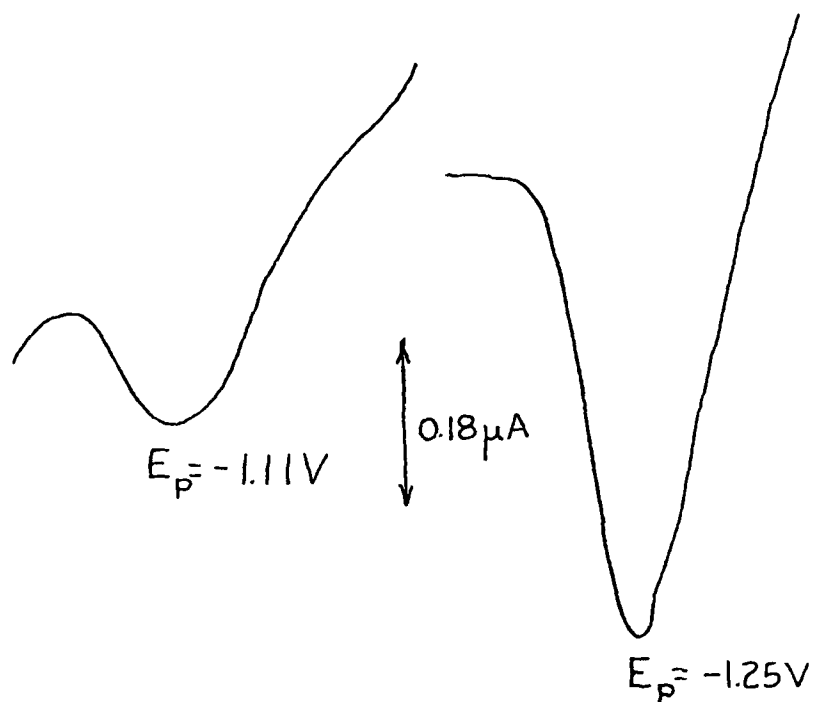
Figure 9.   Comparison of Stripping Peaks Obtained for
            Chromium(III) in Potassium Nitrate and
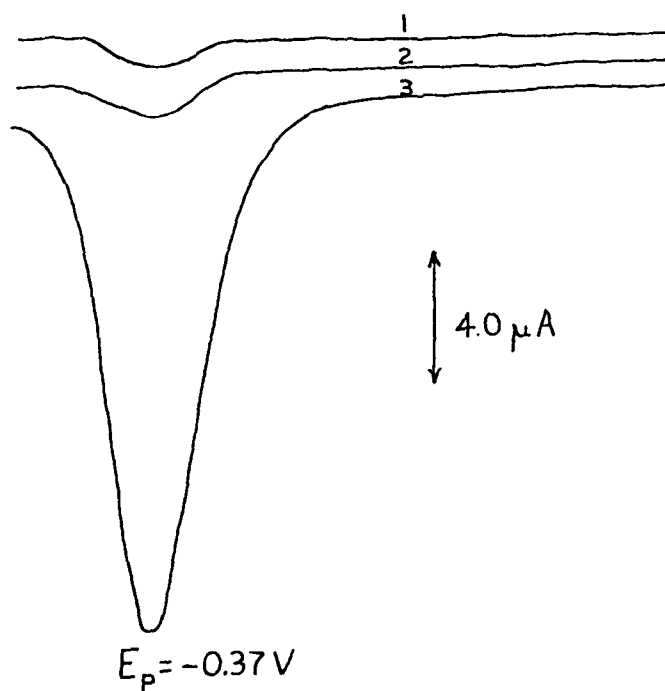   Chromium(III) in Sodium Aceta e.

$E_p = -0.37 \, V$

Figure 10. Effect of Polymeric Film Formation on Peak
Current for Lead(II) in 0.1 F Sodium Acetate
(1) 1 µg/ml of Lead(II)
(2) 2 µg/ml of Lead(II)
(3) 2.5 µg/ml of Lead(II).

polymeric film but the formation is occuring as a phase change owing to the abrupt increase in current observed.

Further work into the effect of surface-active substances on peak current should be done. A study of different sulfur-containing ligands (e.g., those which contain nitrogen donor atoms) may provide a ligand which will strongly chelate chromium(III) or some intermediate oxidation state that may occur during the electrolytic process. If such a ligand were found, and if increases in peak current were to increase smoothly, then the sensitivity of chromium(III) via this ASV technique could be increased several orders of magnitude.

Earlier, sodium acetate was shown to have a favorable effect on stripping peak size and shape. An investigation of this effect along with the use of chromate, CrO_4^{2-}, as a standard in the analysis of chromium is discussed in the next section.

C. The Anodic Stripping Voltammetric Analysis of the Chromium(VI)/Sodium Acetate System

Since the attempt to increase the sensitivity of the ASV analysis of chromium(III) by polymeric film formation failed, the problem of finding a sufficiently sensitive technique remained. In section II-D, the formation of $Cr(OH)_3$ film by the reduction of chromium(VI) at an impregnated graphite electrode was discussed and data for the analysis given in Table 5. The possibility that a similar reaction could occur at a mercury electrode under suitable conditions seemed to be a logical approach to solving the

analysis problem. This section concerns the development of such a technique, the characteristics of the systems involved, applications of the technique to trace analysis, and areas for further research.

Experimentally, the technique is the same as the one used throughout the research. The systems that were used were lead(II) in 0.1 F KNO_3, chromium(III) in 0.1 F KNO_3, and chromium(VI) in 0.1 F NaOAc. Lead(II) was used as a model for comparison and will be discussed first.

Lead is ideally suited to ASV analysis. Lead reacts reversibly with mercury electrodes and is also very soluble in mercury. Lead has been determined by ASV with the hanging mercury drop electrode in sample types ranging from blood and urine to atmospheric particles and sea water. The detection limit for lead by differential pulse and linear scan ASV is 0.01 and 0.02 ng/ml, respectively.[26]

A sample voltammagram for 1 ppm lead(II) in 0.1 F KNO_3 is shown in Figure 11. Notice that the stripping peak is very sharp and well-defined. The sharpness of the peak is indicative of a rapid charge-transfer reaction. From Table 3, the charge-transfer coefficient, α, is 0.94. In general, charge-transfer rate constants and coefficients can be used to a priori assess the feasibility of a particular ASV analysis. If both are large, as in the case of lead, then the analysis should proceed well, whereas small values suggest that the analysis will be more difficult.

Calibration curves, such as the one in Figure 12, give information which can be used to compare different systems.
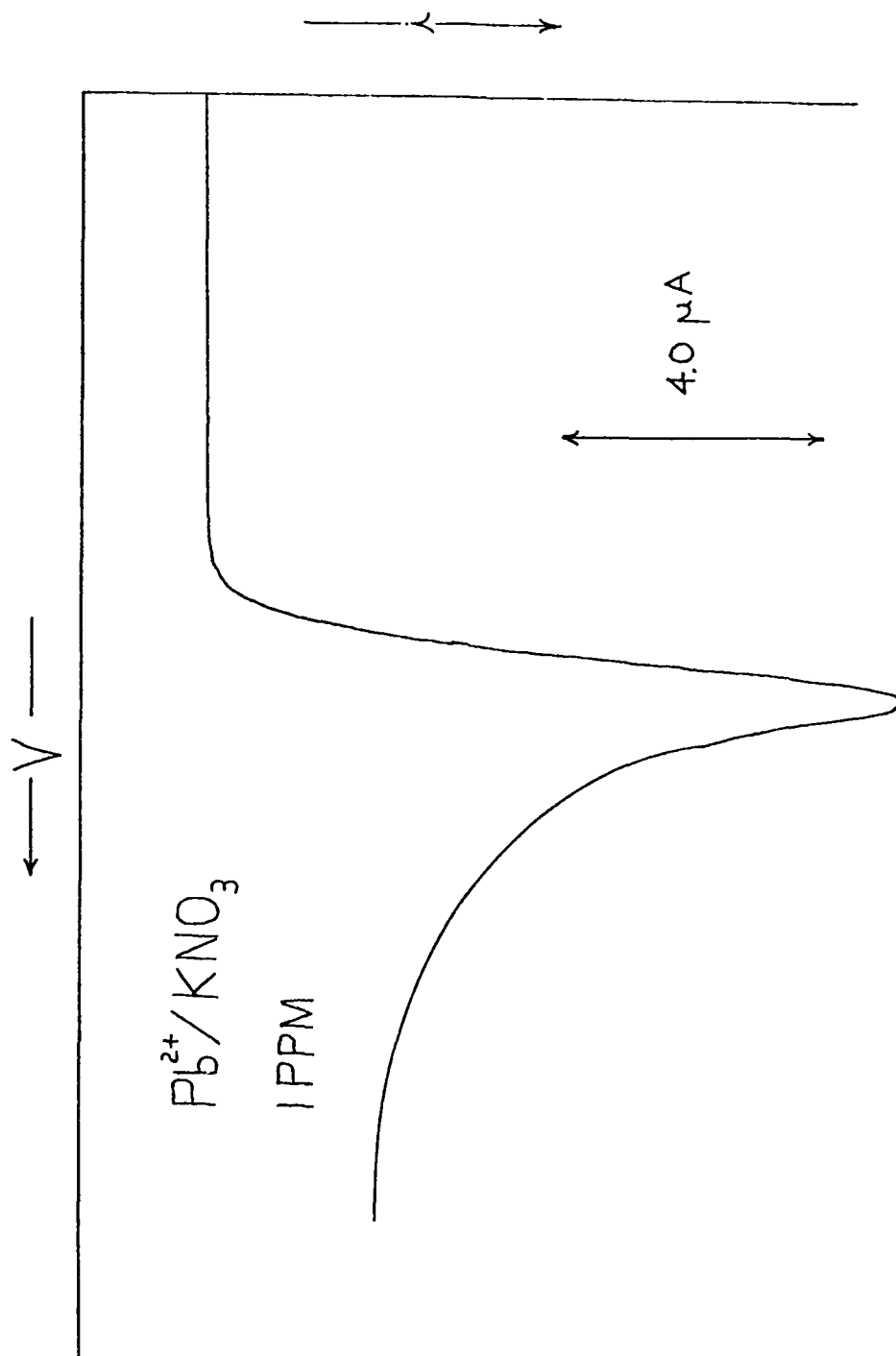
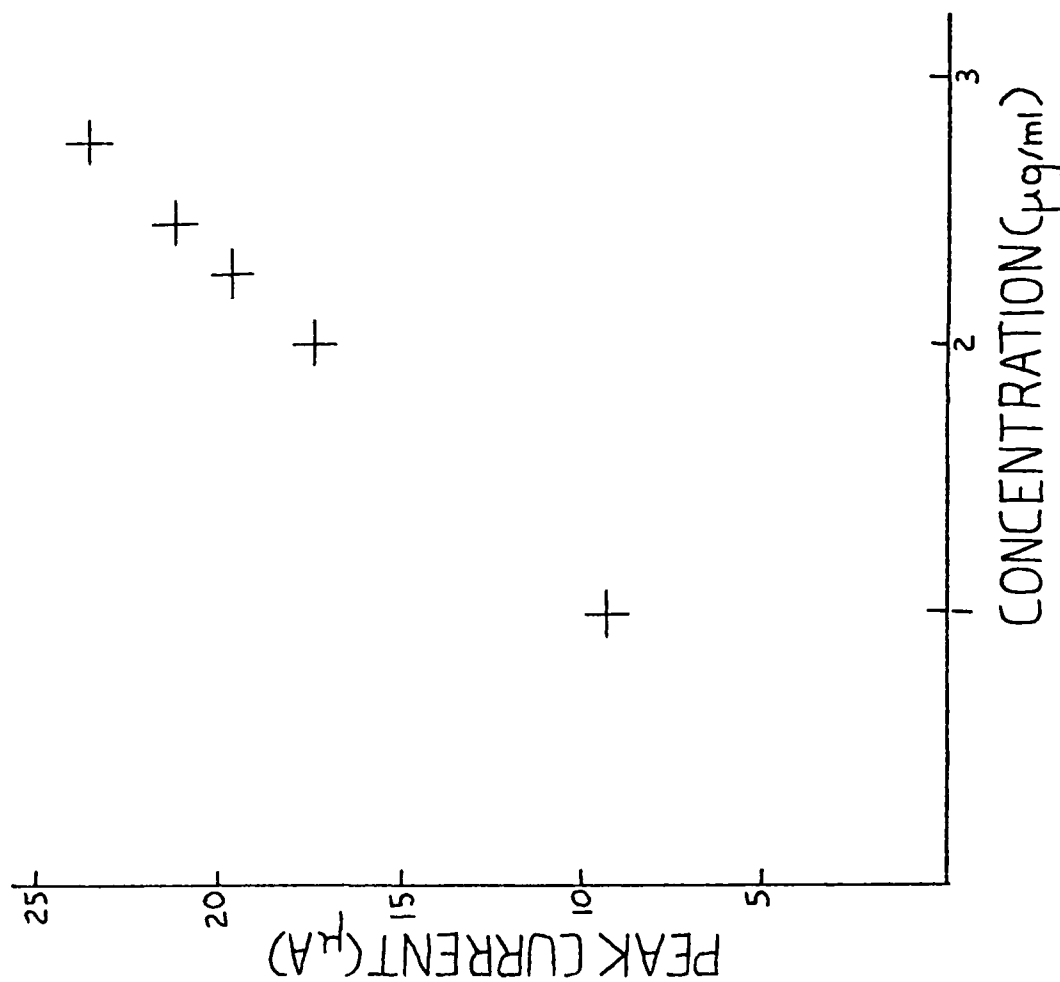Figure 11. Stripping Curve for 1 ppm Pb^{2+} in 0.1 F KNO_3

Figure 12. Calibration Curve for Lead(II) in 0.1 F Potassium Nitrate

The slope of lead's calibration curve is 8.69 µA/µg/ml compared to a slope value of 0.016 for chromium(III) in Figure 6. The amount of signal per unit concentration is much greater for lead. Therefore, slope values can be used for comparing the relative sensitivity of determinations for systems such as lead/KNO_3 and chromium(III)/KNO_3. Also, linearity of the calibration curve is desirable for any ASV analysis.

In contrast to lead, the polarization curve for chromium(III) in 0.1 F KNO_3 (Figure 13) exhibits several undesirable characteristics. For example, the stripping peak of chromium(III) merges on the cathodic side (right side) with the peak which arises from the reduction of hydrogen ion; thus the peak appears somewhat distorted and drawn out. On the anodic side, another smaller peak appears and also causes distortion of the larger peak. This small, broad peak is due to the oxidation of chromium(II) to chromium(III) which is the second step in the overall oxidation of the chromium amalgam to chromium(III). The entire process can be represented as the following oxidation reactions:

$$Cr(Hg) \longrightarrow Cr(II) \longrightarrow Cr(III)$$
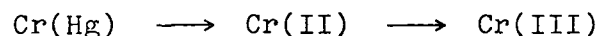
This representation is somewhat simplistic but it is sufficient for now to say that chromium(II) is a somewhat stable, though short-lived, intermediate in the oxidation process. Such behavior was also noticed by L. M. Beasley in an earlier research, although no explanation was given.[27]

When, however, chromium(III) is replaced by chromium(VI) and KNO_3 is replaced by NaOAc, the stripping peak takes on a different appearance as shown in Figure 14. The stripping
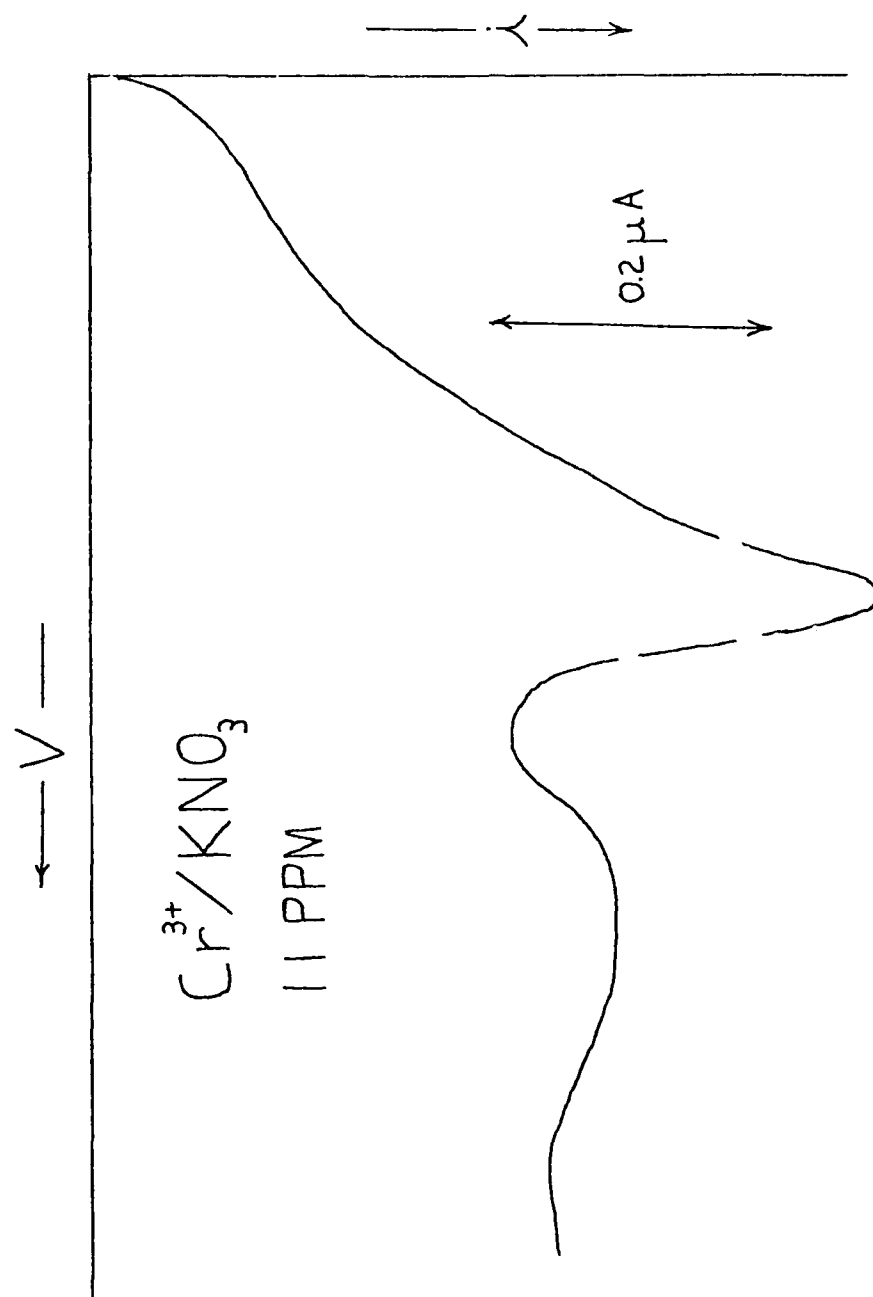
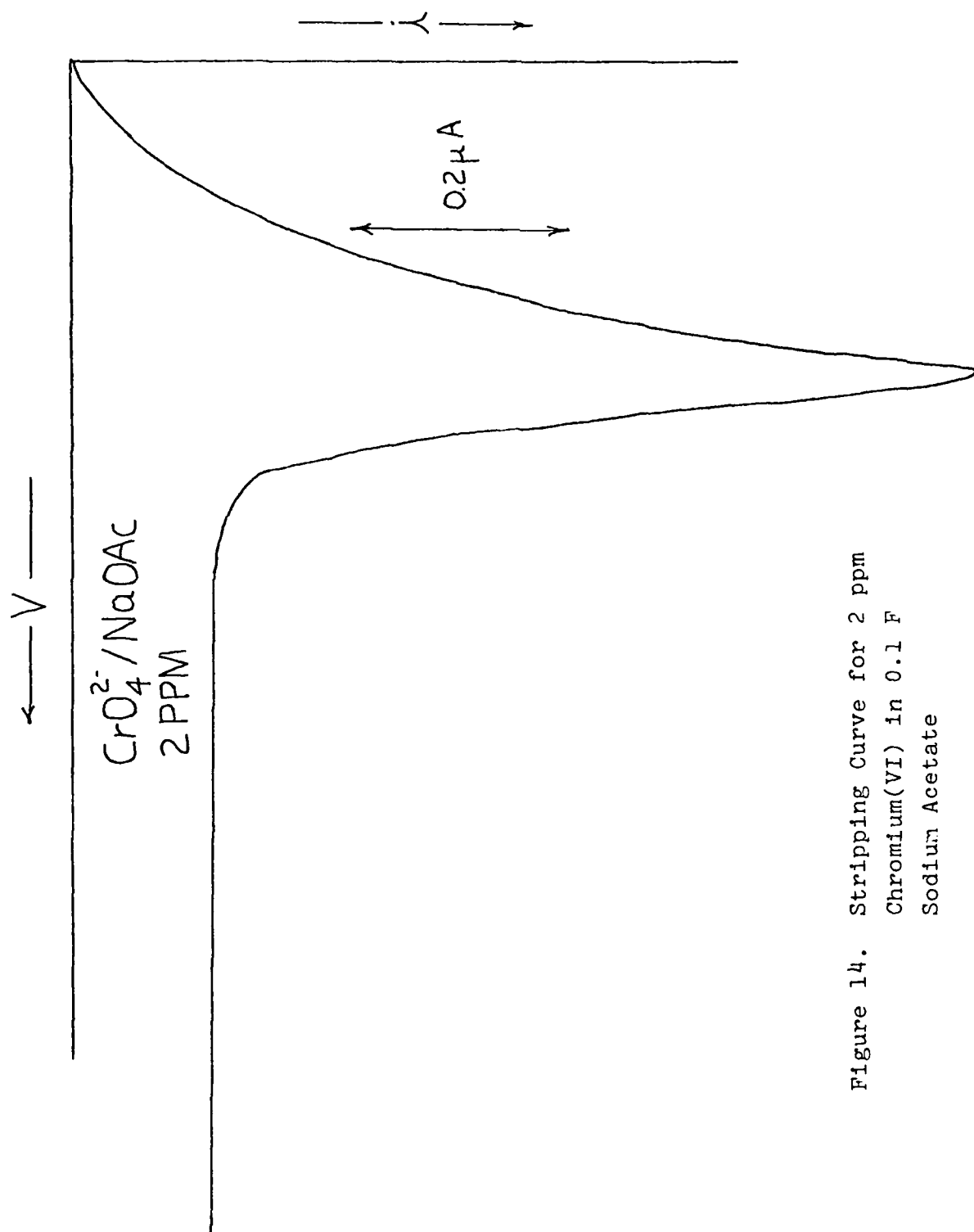Figure 13. Stripping Curve for 11 ppm Chromium(III) in 0.1 F Potassium Nitrate

Figure 14. Stripping Curve for 2 ppm Chromium(VI) in 0.1 F Sodium Acetate

peak current is increased significantly, peak current due to hydrogen evolution is absent, only a single oxidation is observed, and the chromate peak is, in general, sharper and more well defined than the chromium(III) peak. To further characterize the differences between the two systems, cali- bration curves were made up for chromium(VI) and chromium(III) in the concentration range from 1 to 10 µg/ml. The cali- bration curves appear in Figure 15. From looking at the figure, it is obvious that chromium(VI) yields the best calibration curve. In fact, no peak currents were measurable from 0 to 4 µg/ml for the chromium(III)/KNO_3 system. The slope values for the curves are 0.12 and 0.03 µA/µg/ml for chromium(VI) and chromium(III), respectively.

At approximately 7 µg/ml, the chromium(VI) curve begins to flatten out. Repeated runs gave similar results. This upper limit in the determination may be due to the limited surface area of the mercury drop (2.22 mm^2). The assumption that a chromium(III) hydroxide film is formed on the electrode surface seems to be consistent with the observed behavior. The implication is that the mercury drop is saturated with the film and the saturation point is reached at concentrations higher than 7 µg/ml. Concentrations of 1 µg/ml and less were run and the calibration curve appears in Figure 16. The lowest detectable concentration of chromium by this method (using in-house equipment under the specified experimental conditions) appears to be 0.1 µg/ml or on the order of 100 parts per billion.
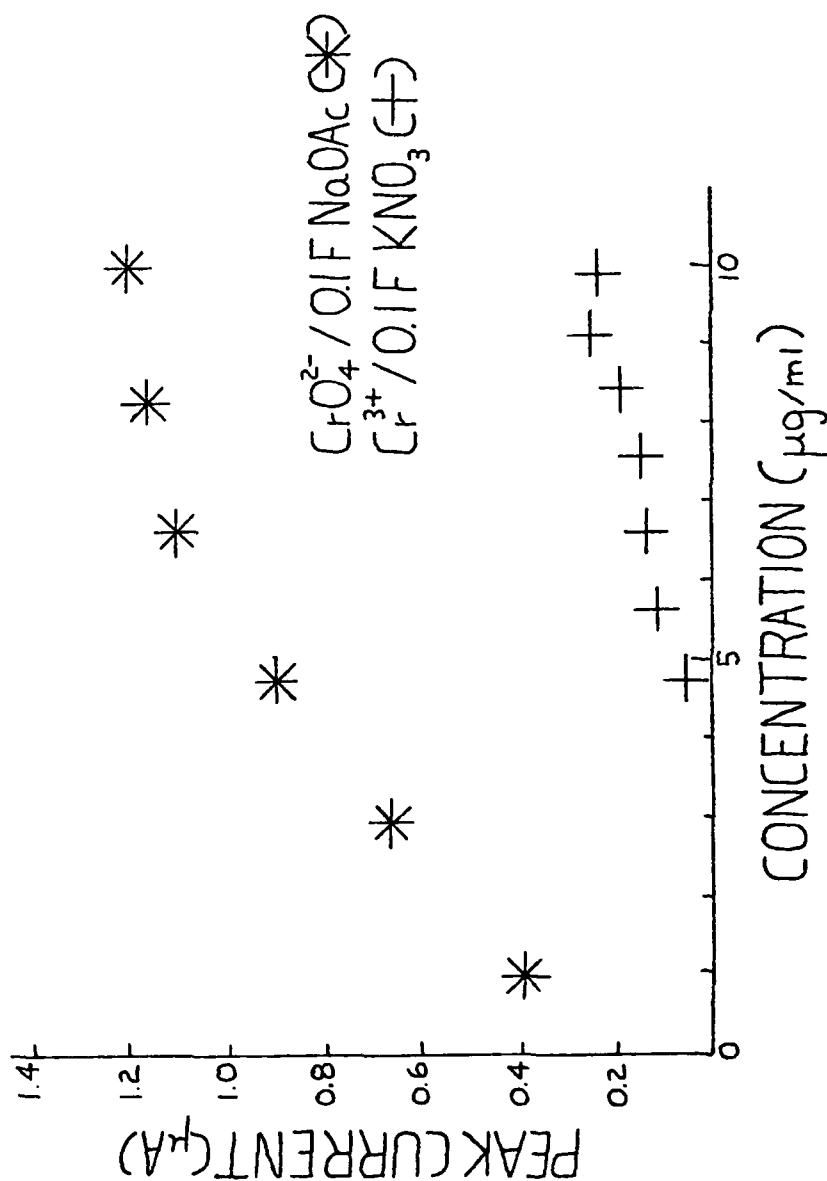
51

Figure 15. Calibration Curves for Chromium(III) and Chromium(VI) in 0.1 F
Potassium Nitrate and 0.1 F Sodium Acetate, respectively.
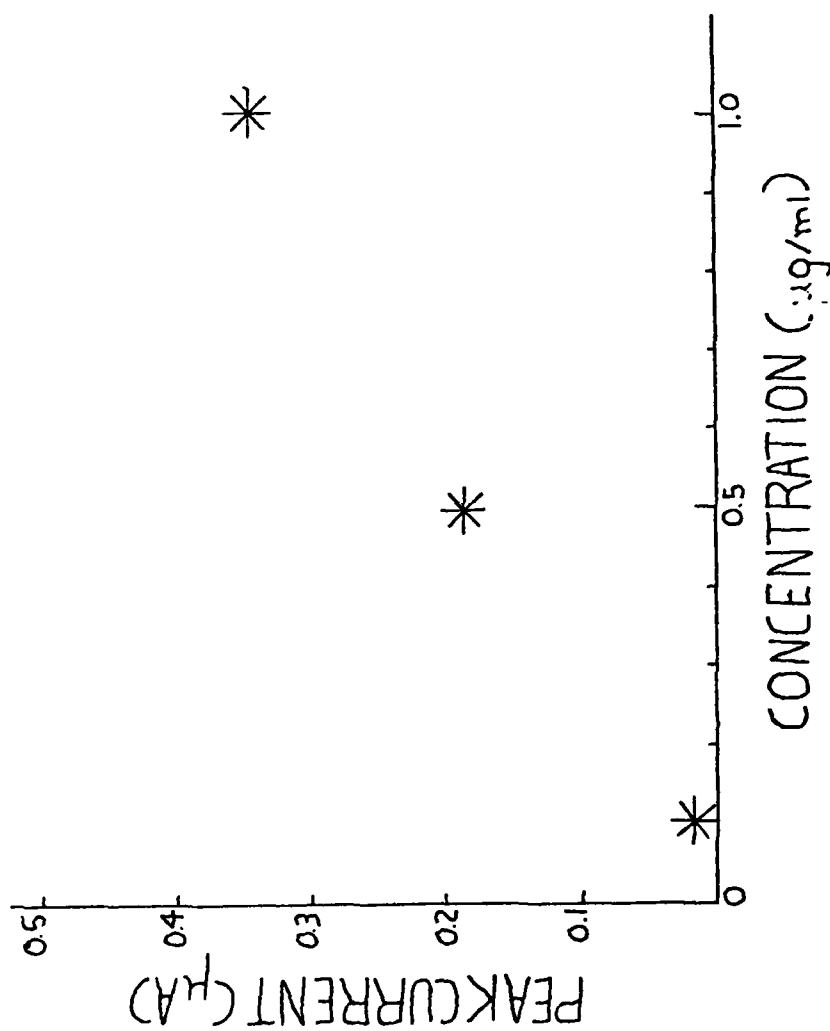
52

Figure 16. Calibration Curve for Chromium(VI) in 0.1 F Sodium Acetate in the Range 0 to 1 µg/ml

The variation of peak potential with concentration was also investigated, and the results are given in Figure 17. The peak potential for chromium(III) varies considerably with concentration, whereas the chromium(VI) peak potential remains constant throughout the concentration range. A constant potential is extremely important in an ASV analysis, especially a multi-elemental analysis where merging of peaks can occur. Consistency of potential is but one more advantage of the chromium(VI)/sodium acetate system. The results of the analysis are given in Table 7.

The large contrasts between the chromium(VI)/sodium acetate and chromium(III)/potassium nitrate systems can, in part, be explained by the difference in pH of the two solutions. As shown earlier, even the chromium(III) peak improves in sodium acetate so that the difference cannot be attributed entirely to the chemical species used. Potassium nitrate is essentially acidic in solution (i.e., pH of 5% solution at 25°C is 5.8), but 0.1 F sodium acetate is slightly basic at 8.83.[28] In neutral or slightly acidic solutions, pre-electrolysis at potentials higher than -1.2 V versus SCE can produce hydrogen ion reduction which will interfere with stripping peaks that occur in the vicinity of -1.0 V versus SCE. However, since 0.1 F sodium acetate is alkaline, the hydrogen ion concentration is lower and the reduction becomes less problematic. Another advantage of sodium acetate's alkalinity is the possibility of chromium(III) hydroxide film formation following the reduction of chromium(VI) to chromium(III).
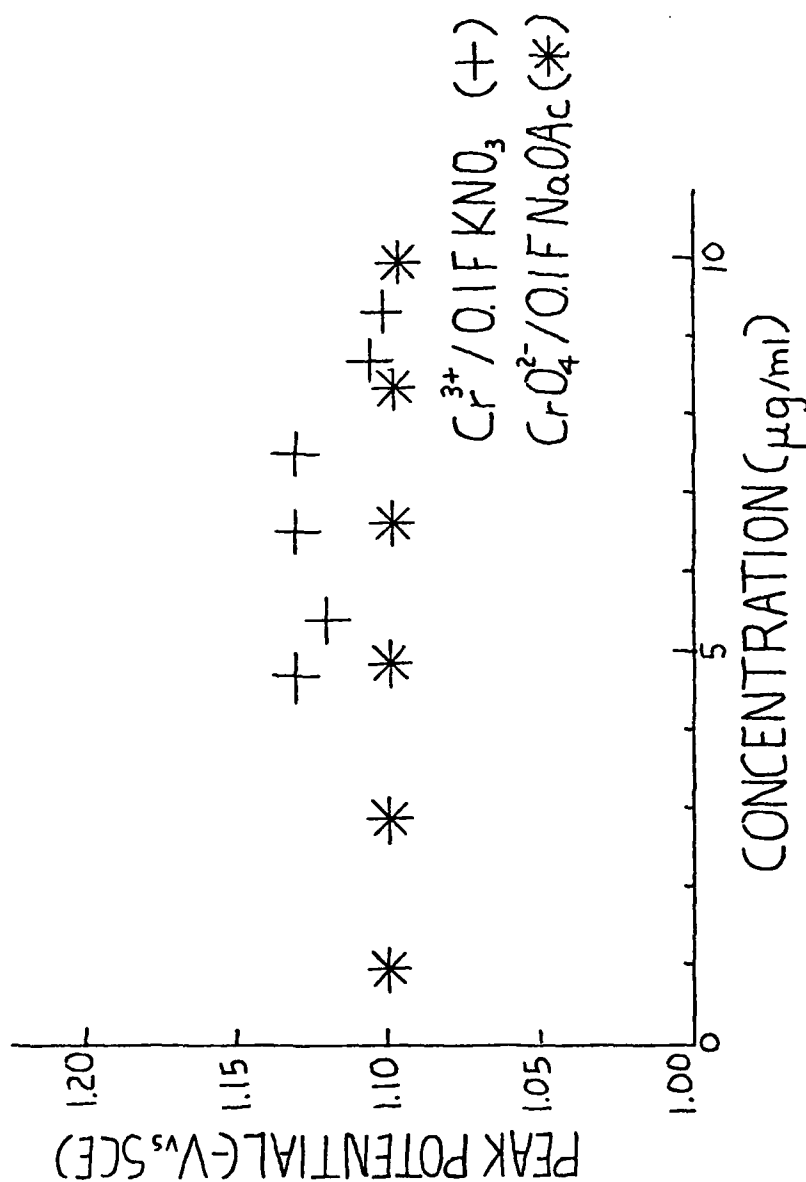
Figure 17. Variation of Peak Potential with Concentration for Chromium(III) and Chromium(VI) in 0.1F Potassium Nitrate and 0.1F Sodium Acetate, Respectively
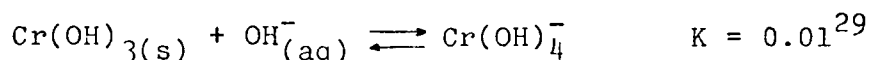
TABLE 7

Representative Data for the ASV Analysis of Chromium

Metal	Concentration (µg/ml)	peak current i_p, (µA)	peak potential $-E_p$ (V vs SCE)	Electrolyte	Calibration curve slope
Pb^{2+}	0	0	0	$0.1F\ KNO_3$	8.69
	0.99	9.20	0.370		
	1.97	17.50	0.370		
	2.22	19.30	0.370		
	2.46	21.15	0.370		
	2.70	23.80	0.370		
Cr^{3+}	0.99	--	--	$0.1F\ KNO_3$	0.03
	1.97	--	--		
	2.93	--	--		
	3.87	--	--		
	4.79	0.04	1.132		
	5.69	0.10	1.125		
	6.58	0.12	1.132		
	7.45	0.13	1.132		
	8.31	0.18	1.115		
	9.15	0.22	1.110		
	9.97	0.21	1.110		
CrO_4^{2-}	0.10	0.01	1.100	$0.1F\ NaOAc$	0.12
	0.50	0.18	1.100		
	1.00	0.34(0.40)	1.100		
	2.91	0.66	1.100		
	4.76	0.90	1.100		
	6.54	1.11	1.100		
	8.27	1.17	1.100		
	9.91	1.22	1.100		

ASV Analysis of Cr^{3+}, CrO_4^{2-}, and Pb^{2+}

$T=22 \pm 0.1°C$, $E_{eL}=-1.4v$ (vs SCE), Scan Rate=50 mv/sec

t=5 min with 30 sec still time

Hg Drop Size: 0.83 mm (DIA), $2.22 \pm 0.07\ mm^2$ (surface area)

In order to say with any degree of certainty whether the conditions are right for the hydroxide film to form, some idea of how alkaline the solution must be in order to achieve minimum solubility of chromium hydroxide must be obtained. A simple way is to calculate the hydroxide ion concentration, convert it to pH, and compare this pH value to the one that's actually used.

The equilibria involved in the calculation are:

$$Cr(OH)_{3(s)} \rightleftharpoons Cr^{3+}_{(aq)} + 3\ OH^-_{(aq)} \qquad K'_{sp} = 7.59 \times 10^{-30}$$

$$Cr(OH)_{3(s)} + OH^-_{(aq)} \rightleftharpoons Cr(OH)^-_4 \qquad K = 0.01^{29}$$
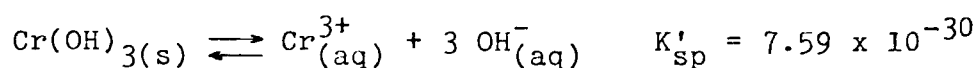
where k'_{sp} is the concentration constant calculated from the solubility product and the activities of chromium(III) and hydroxide ion at an ionic strength of 0.1 mol/l.

From these equilibria, the following equations can be derived:

$$K'_{sp} = 7.59 \times 10^{-30} = [Cr^{3+}][OH^-]^3 \qquad \text{(IV-4)}$$

$$K = 0.01 = [Cr(OH)^-_4]/[OH] \qquad \text{(IV-5)}$$

Rearranging equations (IV-4) and (IV-5) and substituting into the expression for formal concentration, X

$$X = [Cr^{3+}] + [Cr(OH)^-_4] \qquad \text{(IV-6)}$$

results in the following expression for X

$$X = K'_{sp}/[OH^-]^3 + K[OH^-] \qquad \text{(IV-7)}$$

Differentiating equation (IV-7) with respect to the hydroxide ion concentration, setting it equal to zero and solving for the hydroxide ion concentration yields

$$[OH^-] = \sqrt[4]{\frac{3K'_{sp}}{K}} = 2.18 \times 10^{-7} \text{ mol/l}$$

Therefore, a solution pH of 7.34 is required and is within one and a half pH units of the 0.1 F sodium acetate solution used in the analysis. This strongly suggests favorable conditions for hydroxide film formation.

The upper limit of detection has already been explained in terms of the limited surface area of the mercury drop. The lower limit of detection may be due to the solubility, however small, of chromium(III) hydroxide in the 0.1 F sodium acetate solution. In other words, as the concentration of chromium(VI) and--therefore the chromium hydroxide--becomes smaller and smaller, the chromium hydroxide may at some point remain in solution as separate ions rather than precipitating as the hydroxide film.

The solubility of chromium(III) hydroxide can be determined by calculation. The equation for the formation of the chromium hydroxide is

$$Cr(OH)_{3(s)} \rightleftharpoons Cr^{3+}_{(aq)} + 3 OH^-_{(aq)}$$
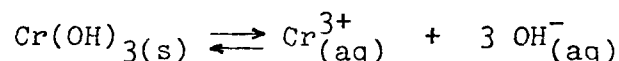
and the concentration constant, K'_{sp}, is defined by equation (IV-4). Setting the concentration of chromium(III) equal to X mol/l and the concentration of the hydroxide ion equal to 3X mol/l yields

$$K'_{sp} = 7.59 \times 10^{-30} = [Cr^{3+}][OH^-]^3 = 27X^4$$
$$\text{and } X = 2.3 \times 10^{-8} \text{ mol/l}$$

Therefore, the solubility of chromium(III) hydroxide in 0.1 F sodium acetate is on the order of two parts per billion and

should represent the theoretical detection limit. This value
is about two orders of magnitude lower than the experimen-
tal detection limit. The difference between the two may be
due to the inherent limitations of the instrumentation,
charging currents associated with the double-layer and large
scan rates, the IR drop in solution, etc.

Additional information regarding the nature of the
electrolytic process involved in the analysis of chromium
was gained in a dc polarographic study of chromium(VI),
chromium(III), and lead(II). Polarograms of each are shown
in Figure 18. Lead(II), again, exhibits fast, reversible
reduction as evidenced by the sharp increase in diffusion
current as the half-wave potential is approached. No further
reductions occur and the single reduction observed involves
the formation of the lead amalgam. Chromium(III) exhibits
two reductions in the potential range from about -1.0 to
-1.4 volts versus SCE. The more anodic reduction involves
the reduction of chromium(III) to chromium(II), the reduction
counterpart of the ASV peak which appears in the voltamma-
gram for chromium(III) in Figure 13. The reduction at
$E_{\frac{1}{2}}$ = -1.5 volts versus SCE corresponds to the reduction of
the chromium(II) species, generated by the previous reduction,
to the sparingly soluble chromium amalgam. Notice, however,
that the chromium polarogram is more drawn out along the
potential axis as compared to lead and suggests a slower rate
of charge-transfer. The half-wave potentials for chromium(III)
in 0.1 F potassium nitrate are roughly equivalent to those
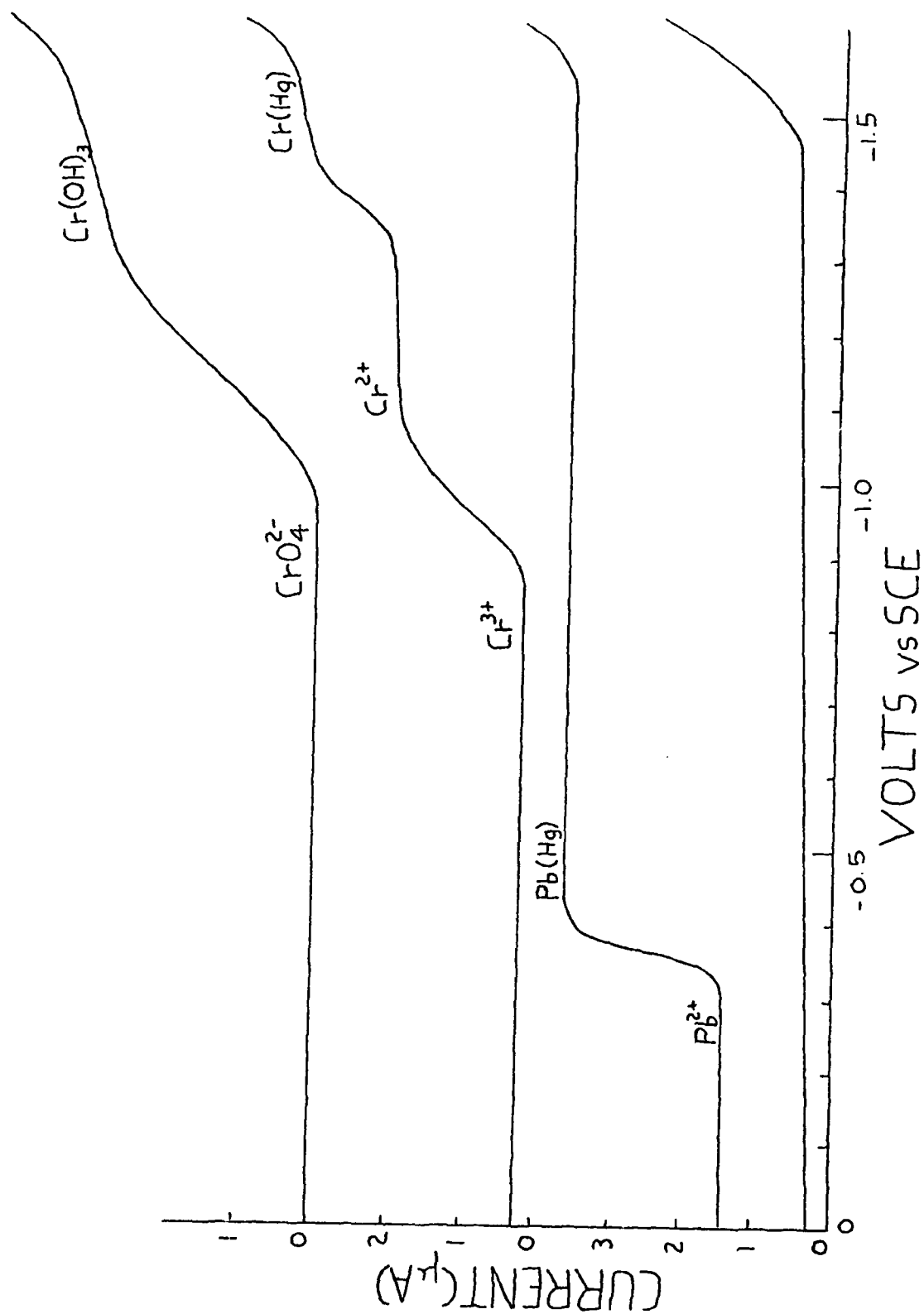listed for $Cr(H_2O)_6^{3+}/K_2SO_4$ in Table 4. Chromium(VI) in 0.1 F

59

Figure 18. DME Polarograms of $10^{-3}M$ Pb^{2+}, Cr^{3+}, and CrO_4^{2-} in 0.1 F KNO_3, 0.1 F KNO_3 and 0.1 F NaOAc, respectively

sodium acetate yields only one reduction in contrast to chromium(III) and parallels the polarization curve for chromium(VI) shown in Figure 14. Again, the postulation of hydroxide film formation seems to be corroborated. Comparison of half-wave potentials for chromium(VI) in sodium acetate ($E_{\frac{1}{2}}$ = -1.30 volts vs SCE) and in potassium hydroxide ($E_{\frac{1}{2}}$ = -1.03 volts vs SCE) as contained in Table 4 show some agreement. Data for the polarographic study is contained in Table 8.

As a final argument for hydroxide film formation, consider the situation where chromate is reduced to the metal amalgam. Such a reduction would involve chromium(II) as an intermediate that would probably appear in either the polarogram or voltammagram of chromate. It has been shown that it does not. Also, reduction to the metal would still involve a chromium-mercury solubility problem, and the analysis would be back at square one. These considerations, along with data provided, seem to lend credence to the hydroxide film explanation.

Any ASV analysis must include a consideration of potential interferences by other commonly analyzed metals. The four metals most commonly analyzed by ASV are Cu, Pb, Cd, and Zn. Standards of these metal salts were prepared from Harleco (1000 ppm) atomic absorption standards. A sample voltammagram of Cu, Pb, Cd, and CrO_4^{2-} is shown in Figure 19. Cu, Pb, and Cd at concentrations nearly three times that of chromium(VI) did not interfere. Zinc, however, was found to interfere due to the occurence of its peak

TABLE 8

Comparison of Peak Potentials (versus SCE) versus

Half-Wave Potentials for Lead(II),

Chromium(III), and Chromium(VI)

Metal	E_p(volts)	$E_{\frac{1}{2}}$(volts)	Electrolyte
Lead(II)	-0.370	-0.395	0.1F KNO_3
Chromium(III)	-1.122*	-1.500**	0.1F KNO_3
Chromium(VI)	-1.100	-1.330	0.1F NaOAc

* Calculated average of seven values
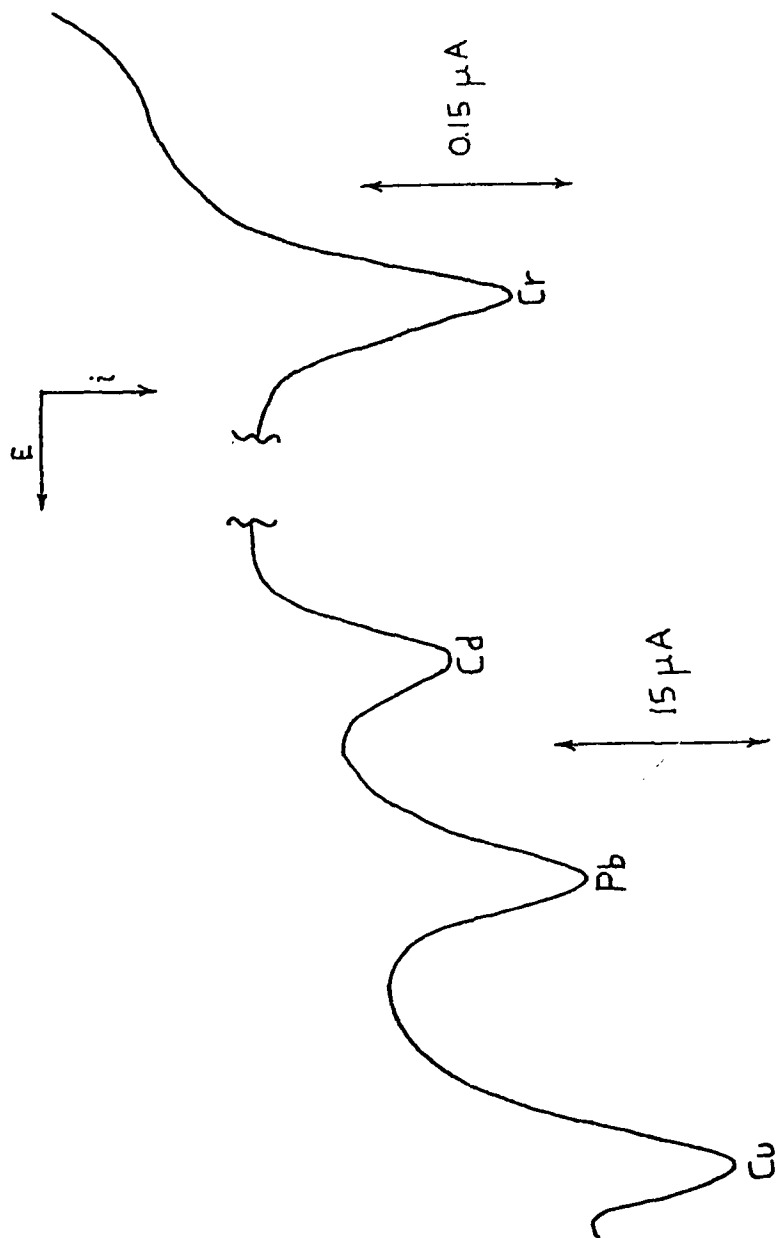
**Estimated value

Figure 19. Stripping Curve for 2.5 ppm Copper(II), Cadmium(II), Lead(II), and 1 ppm Chromium(VI) in 0.1 F Sodium Acetate

potential at -1.0 volts vs SCE which merges with the strip-
ping peak for chromium(VI). Elimination of the zinc inter-
ference may be possible by performing a preliminary separation.
An ammonia-ammonium chloride buffer is perhaps the most common
medium employed for separation of iron, chromium, aluminum
and titanium from manganese(II) and the alkaline-earth
hydroxides. Copper, zinc, nickel and cobalt form stable
ammine complexes and also remain in solution. The precipitates
formed in this environment are frequently gelatinous and
difficult to manipulate. Moreover, as a result of surface
adsorption, they tend to carry down substantial amounts of
the ions in solution.[30]

Chromium analysis with the HMDE by the chromium(VI)/
sodium acetate method seems to be a very convenient method
to determine at least part per million concentrations of
chromium. Now, perhaps chromium can be added to those ele-
ments which are currently "easily" determined by ASV as
shown in Figure 20. Certainly more work must be done,
particularly on "real world" samples where the matrix is
much more complicated and pre-treatment of the sample may
comprise the largest and most arduous part of the analysis.
Specifically, chromium may exist in several oxidation states
in the original sample. Oxidation to chromium(VI) by
ammonium peroxydisulfate with silver nitrate as a catalyst
may prove to be an acceptable procedure. Certainly, the
detection limit may be improved, perhaps by acquiring a new
measuring circuit. For example, a differential pulse circuit
may conceivably lower the detection limit by an order of

Figure 20.   Elements Determined by Stripping
Voltammetry[31]

magnitude. The upper limit of detection may also be improved by using a thin-film mercury electrode (TFME) having a much larger surface area than the hanging mercury drop electrode. Thus, more of the hydroxide film could be deposited on the electrode (effecting an increased capability for detecting higher concentrations of chromium) without giving up the advantages of a mercury electrode.

In summary, the tools are available for trace analysis of chromium with mercury electrodes and the need for such an analysis is very real. Chromium is an important constituent in our diet, and chromate dusts have been shown to be carcinogenic. In such areas as these, I hope that this work can, in some small way, make the analysis of chromium a simpler, and in these days of budget cuts, a less expensive task.

BIBLIOGRAPHY

1. F. Vydra, K. Stulik, and E. Julakova, "Electrochemical Stripping Analysis," Halsted Press/John Wiley & Sons, Inc., New York, N.Y. (1976) pp. 15-19.

2. Reference 1, p. 36.

3. W. Nernst, Z. Physik. Chem., 47, 52 (1904). Reference 1 summarizes this work.

4. V. S. Bagotski and Yu V. Vasiter, "Fuel Cells: Their Electrochemical Kinetics," Consultants Bureau, New York (1966). Reference 1 summarizes this work.

5. Z. Samec and J. Weber, J. Electroanal. Chem., 38, 115 (1972).

6. V. G. Levich "Physicochemical Hydrodynamics," Prentice-Hall, Englewood Cliffs, New Jersey (1962). Reference 1 summarizes this work.

7. Reference 1, pp. 37-38.

8. W. H. Reinmuth, Anal. Chem., 33, 185 (1961).

9. W. H. Reinmuth, J. Am. Chem. Soc., 79, 6358 (1957).

10. I. Shain and J. Lewinson, Anal. Chem., 33, 187 (1961).

11. M. T. Kozlouski, A. I. Zebreva, and V. P. Gladyshev, "Amalgamy i ikh Primenenic, Izd," Nauka, Alma-Ata (1971). Reference 1 summarizes this work.

12. A. Regner, "Technicka' Electrochemie," Academia Progue (1967). Reference 1 summarizes this work.

13. G. Jangg and H. Kirchmayr, Z. Chem., 3, 47 (1963). Reference 1 summarizes this work.

14. J.E.B. Randles and K. W. Somerton, Trans. Faraday Soc., 48, 951 (1952).

15. G. C. Barker, R. L. Faircloth and A. W. Gardner, Nature, 181, 247 (1958).

16. P. Delahay and A. Aramata, J. Phys. Chem., 66, 2208 (1962).

17. W. Kemula, Z. Galus and Z. Kublik, Nature, 182, 1228 (1958).

18. F. von Sturm and M. Ressel, Z. Anal. Chem., 186, 63
     (1962). Reference 1 summarizes this work.

19. J. Heyrovsky' and P. Zuman, "Practical Polarography,"
     Academic Press, New York, N.Y. (1968) p. 191.

20. M. von Sway and R. S. Deelders, Nature, 191, 241 (1961).

21. L. A. Krapiokina and Kh. Z. Brainina, Zavodsk. Lab.
     33, 400 (1967). Reference 1 summarizes this work.

22. L. M. Beasley, "The Effects of Bridging Ligands on
     Anodic Stripping Voltammetric Analysis," Master's Thesis,
     Western Kentucky University, p. 36.

23. Inverse Polarography (anodic stripping) operating
     instructions, Metrohm Herisau, Switzerland.

24. R. Neeb and I. Kiehnast, Z. Anal. Chem., 226, 153 (1967).

25. B. A. Parkinson and F. C. Anson, Anal. Chem., 50, 1886
     (1978).

26. T. R. Copeland and R. K. Skogerboe, Anal. Chem., 46,
     1257A (1974).

27. Reference 22, p. 61.

28. D. A. Skoog and D. M. West, "Fundamentals of Analytical
     Chemistry," Holt, Rhinehart and Winston, Inc., New York,
     N.Y. (1969) p. 254.

29. E. H. Swift and W. P. Schaefer, "Qualitative Elemental
     Analysis," W. H. Freeman and Company, San Francisco,
     CA, (1962) p. 446.

30. E. H. Swift, "A System of Chemical Analysis," W. H.
     Freeman and Company, San Francisco, CA (1938)
     pp. 284-285.

31. F.P.J. Cahill, G. W. VanLoon, American Laboratory,
     Aug. (1976) p. 11.